Point by point response to reviewers and list of relevant changes:

Reply to Referee #2:

The revised manuscript does not meet my expectation. The authors only changed the title while I asked for substantial changes in their discussion. Their conclusions that 1) phytoplankton abundances changed over time and space, 2) results from a flow cytometer and fluorimeter are correlated, 3) more sampling enable more matches up with satellite, does not really represent a scientific progress in my opinion.

I also suggested more details about the PHYSAT methods and results, and suggest to reduce the number of figures and shorten the length of the manuscript. None of these recommendations were considered. As this point, I can not recommend this paper for publication.

Reply (authors reply in italic)

We thank the reviewer for its critical point of view, which help us to improve our paper. We do add some information about PHYSAT method in addition to references to past publications. Furthermore, we would like to comment point by point about arguments resulting in the reviewer rejection of the revised version of the manuscript in order to explain our choice.

1. Phytoplankton abundances changed over time and space

First, we would like to remind the reviewer of the necessity of both qualitative and quantitative description of any community changes over time and space in any ecological study. Indeed, marine ecology refers on community structure and heterogeneity. It is based on community description (either in terms of species or ecological functional groups) through abundances, biomass, distribution and change in time. The current paper is one of the first paper describing phytoplankton structure at the functional trait level and at the frequency of

one sample every hour in surface waters in the North Sea for 5 entire days. To ensure high quality dataset, phytoplankton dynamics is adequately observed only by sampling at the frequency resolving its intrinsic changes, i.e. at the sub mesoscale and the hourly scale. As it is hardly possible to meet both, current advances in technology (cytometry and remote sensing) make it nearly possible to reach the sampling frequency and the resolution accuracy needed. Such a high level of resolution is reached for the first time thanks to the co evolution between researcher's knowledge and technologies advances. This paper is part of it.

The presentation of the phytoplankton distribution, size classes and contribution to chlorophyll (which, although not being the best indicator of biomass, is unfortunately still used by most of the biogeochemical models) for each phytoplankton functional group is a serious step forward in understanding its role in its habitat, and further will fill the gap of understanding marine ecology processes.

From the author's point of view, it is not acceptable to submit a paper about phytoplankton community structure and spatio-temporal heterogeneity without describing abundances, size and "biomass" changes. Although the description and discussion about the phytoplankton community composition and distribution makes the paper longer, we argue that it's an essential part. Skip it would mean that cluster's identification in terms of species or genus from flow cytometry was already validated while it is not.

2. results from a flow cytometer and fluorimeter are correlated

This part of the manuscript evidences that the different techniques used to describe the phytoplankton from either remote sensing and in situ sensors are measuring the similar quantity. This is of importance since the multiplication of instruments sold to measure either bulk chlorophyll or size structure leads to a need of coincident evaluation. This also evidences the power of SFC in resolving the entire phytoplankton community instead of the bulk

chlorophyll level which has been used since several decades, but providing limited information on marine ecological processes.

Furthermore, summing up each single cell red fluorescence shape is a way to compare the empirical link of each phytoplankton group to PHYSAT anomalies instead of abundances as it was done before. The fact that the values are comparable to the bulk chlorophyll a means we can use this proxy as a descriptor of each phytoplankton group contribution and associate it to its remote sensing signature.

3. more sampling enable more matches up with satellite

This sentence is not the main part of the discussion, but indeed takes too much place in the last paragraph as a conclusion. The conclusion was modified as follows:

In conclusion, phytoplankton community distribution resolved at the sub mesoscale evidence the importance of the North Sea hydrological context. Significant differences between the two sets of communities observed during the sampling period are mainly due to cryptophyte like cells and bellow nanophytoplankton size class cells. This daily scale resolution thanks to high resolution techniques meeting single cell and remote technologies will help in understanding the role of circulation and hydrological properties of the water masses on the phytoplankton composition, succession schema, spreading and bloom triggering and collapsing.

I also suggested more details about the PHYSAT methods and results, and suggest reducing the number of figures and shortening the length of the manuscript. None of these recommendations were considered. As this point, I cannot recommend this paper for publication.

More details about PHYSAT were added and figures (maps) have been improved in term of color contrast. The additional text is highlighted in the manuscript, which becomes longer. The authors apologize for this but admit that potential readers of our paper are not necessarily specialists of remote sensed approaches or don't have sufficient time to read past papers. However, we would like to point out that PHYSAT is published for more than ten years now and have been cited in more than 140 published papers. So, it's not usual to explain it again and again in details. However, we accept it by considering the multidisciplinary approach of our work (which is, in our view, also a good thing).

It is hardly possible to decrease the size of the manuscript without skipping phytoplankton high resolution description. Since this part of the paper is of importance to understand its ecological role in the studied area, we chose to not remove it. As any paper dealing with flow cytometry, especially with high frequency analysis, describing phytoplankton community is long and fastidious, but we find this fundamental. We could have chosen to focus our paper on community structure description (diel changes, statistical multivariate analysis, etc) but did not chose this way for this paper considering the future huge potential of coupling such in situ measurements with remote sensing observations. We would like to emphasis again on the fact that this is the first time that such a combination was done with successful results, and we find it sufficient to justify a paper in itself.

Considering the request to make substantial changes in the discussion, we do not want to go too far in conclusions that could be done based on such results since they are only describing the community over one week, although at a very high resolution. At this stage, we argue that it wouldn't have been rigorous to describe the role of phytoplankton at the North Sea basin scale with only one week of data.

Reply to referee #3

Mis en forme : Police :(Par défaut) Arial, 14 pt

This is my second review of the manuscript by Thyssen et al. The manuscript has been slightly improved while the answers to my review have been somewhat disappointing, for 2 reasons.

First, it appears that the authors have for some reasons not worked on many of my secondary comments, going from the main comments to those associated with page 15639 (almost the end of the first draft), skipping all the material in between. I have made the effort to repeat all these comments with updated line numbers. Most deal with wording and minor clarifications (see below).

Reply:

We seriously apologize for this mistake and did not will to skip the referee's comments. The own explanation would be that it may be an error in copy past from the original pdf file.

We are going to respond step by step to the first and the second referee's review. Thank you for this very useful and precise work on our manuscript.

Second, some of my main comments seem to have been interpreted as a request to add a lot more about the PHYSAT approach or about flow cytometry, which is a misunderstanding. I fully understand that the authors do not want to enter into details on these topics; this is indeed not needed, nor requested. My comments suggested the possibility of adding just a little bit of text to ease the understanding of the manuscript by non-experts. I still think that defining Ra with its equation would help non-experts in optics to grasp what PHYSAT is

about, that splitting the almost monolithic Section 2.1 into paragraphs with a couple of introductory sentences here or there would help non-experts in cytometry. I as well think that recalling in the discussion that non-phytoplankton material (e.g., sediments) can contribute to the differences in optical properties observed between clusters is appropriate, and that showing nLw spectra (and not only the anomalies) is interesting. Again, these points do not imply anything about PHYSAT's developments. Same thing for my comment on Figure 12 (it was just about colors… but I have bad eyesight).

Reply:

Thank you for these clarifications. Information about PHYSAT and Ra were added in the manuscript, although we do not want to increase the size of the manuscript by adding the equation of the Ra definition.

Furthermore, we split paragraph 2.1 into two parts in order to make it easier to understand for non-specialists.

The Vantrepotte et al. classification for non-turbid waters minimizes the impact of CDOM within the coastal waters (class 1 and 2 of the referred paper). Sediments are supposed to have very little impact on those classified waters which were used for the PHYSAT pixels selection. The sentence in the Material and Method paragraph was modified to make it clear:

"The effects of sediments and/or CDOM were minimized by focusing on phytoplankton dominated waters as defined from the optical typology described in Vantrepotte et al (2012)."

Ultimately, while I'm leaving the decision to the authors, I would encourage them to consider

taking these comments into account, in order to make the manuscript more readable and complete. I'd also recommend to act on the secondary comments below.

Abstract

l.30: "spatial"

l.44: "chlorophyll-a" (or 'a' in italic).

l.47: I'd remove "classical"

l.48: "and remote sensing"

Reply: done

Introduction

l.69: "such a proxy"

l.70: "does not"

l.78: define DMSP at first use

Reply: done

l.79: the last properties, thug relevant for the biogeochemical cycles are not directly linked to the elemental cycles.

Reply: yes indeed, size classes is a good enough functional trait for the description of the food chain

l.91: I'd suggest: "algorithms applied to remote sensing data".

l.107: I'd start a new paragraph after "available".

l.111: "It is critical to understanding…" I'd say.

l.126-127: “in situ data describing phytoplankton …”

l.128: “with a totally”

l.137: “significantly distinct” ?

l.138: “the case in/with”

Reply: done

Section 2.1

The use of several paragraphs would help in making the description of methods clearer.

Reply: done. Two paragraphs were created in this section.

l.160: “1-10 cm3 of seawater”

l.171: the acronym PMT may defined here (it is used afterwards).

l.172: are the 2 trigger levels associated with the 2 photomultipliers?

Reply: Indeed, the two trigger levels were applied only on the high sensitivity PMT and this was defined in the section.

l.174: “less concentrated”

l.195: “above this value” ? I think I understand the sentence but it is not well written.

Reply: The High sensitivity PMT behaved linearly with the low sensitivity PMT until the high sensitivity PMT reaches its saturation level (4000 mV). The linear behavior between those two sensors enables to retrieve the high sensitivity PMT based on the extrapolation from the non-saturating signal of the low sensitivity PMT. The sentence was modified as follow:

"The TFLR signal was corrected from high sensitivity PMT saturation signal in the case of highly fluorescing cells (> 4000 mV) thanks to the low sensitivity PMTs that behaved linearly with the high sensitivity PMT, allowing the reconstruction of the high sensitivity signal."

l.199: "pre-determined": not clear what this means at this stage.

Reply: The sentence was changed in order to be clear:

"The amount of pictures was determined before each sample acquisition and pictures were randomly collected within the largest particles until the predetermined number of pictures was reached."

Section 2.2

l.204: "ship's seawater" ?

l.212: MODIS on-board Aqua I guess

l.225: please correct this sentence. Are the data Level-2 or Level-3? (the latter if they are 4-km data).

Reply: In order to make it clear, the sentence was modified.
"MODIS chla values corresponded to Level-3 binned data consisting of the accumulated daily Level-2 data with a 4.6 km resolution."

l.233: MLD is not a temperature difference… I'd suggest: "defined as the depth associated with an observed temperature difference of more than 0.2C with respect to the surface…"

Reply: done

Section 2.5

l.237: "remotely sensed"

l.241: "aerosol optical thickness" I guess

Reply: Yes indeed, the term aerosol was added.

l.243-244: “coastal areas, that are not considered as open waters for remote sensing”: this sounds awkward; remote sensing (of ocean color) responds to optical properties.

Reply: Indeed, the sentence was changed in order to be clear:

“*In addition, we have selected pixels according to their optical properties following Vantrepotte et al. (2012) criteria in order to keep only waters corresponding to open water signature*.”

l.255: “radiance”? “anomaly spectra”

Reply: The sentence was omitted since it was defined in the PHYSAT description as requested by the Reviewer 2.

Section 2.6

l.260: “normality was not applied”: is “applied” really the proper word here?

Reply: It was changed to “When data did not follow a normal distribution,”

l.264: “remotely”

Section 3.1

l.277: “four … zones” ?

l.278: “associated with”

l.279: “samples varying between...” ? (the sentence is currently incorrect).

l.290: “3 E” ?

Reply: done

Section 3.2

l.297: repeating “cluster” each time may not be necessary

l.301: “within the Micro2 cluster”: what about the other clusters? Is it related to size?

Reply: Indeed, Micro2 is related to size and the other cluster’s names are also related to size (Pico/Nano/Micro). The description of Micro2 was deleted in order to be coherent with the other cluster’s nomination.

l.303-304: “25 pictures collected within 47 counted cells”: what does it mean exactly? Is it random or related to a choice or size?

Reply: The pictures are collected one after the other within a predefined area or cluster until it reached the amount of requested pictures. When it is said that 25 pictures are collected within 47 counted cells means that the user requested 25 pictures within the cluster but that 47 cells were counted within this cluster during the analysis.

Section 3.4

l.359: “remotely”

l.363-365: this further selection is not clear to me.

Reply: the sentence was modified in order to clarify:

"Additional samples collected out of this period results in the loss of correlation significance between MODIS chla and the AOA fluorometer chla within the SFC dataset (r=0.49, p=0.06, n=15, Spearman rank test), leaving 15 SFC matching points (Fig. 1 and Fig. 8)."

l.393: "associated with"

l.395: synthesis": do the authors mean 'composite'?

Reply: Yes

l.397: "tongue"?

Reply: Done

Section 4

l.404: "spatial"

l.413: "SFC" ?

l.427: "which is needed"

l.432: "taxonomic"

l.433: the use of "although" is incorrect here.

l.446: "possibly related" ? "taxonomic"

Reply: done

l.465: "inter-bloom": please specify what that refers to.

Reply: A sentence was added in brackets to clarify: "(haploid stage, life stage persisting between two blooms of diploid colonial cells)"

l.470: "… fell when…": considering what's said before, this sounds contradictory.

Reply: The sentence was modified as follow:" Their presence suggested an area of Phaeocystis colonial blooming stage (Guiselin 2010). "

l.476: "diffusing"? do the authors mean "scattering"?

Reply: Yes

Fig.3: I would specific in the legend that the colors are consistent across the different panels.

Reply: *Done*

Fig.12: my comment here had nothing to do with PHYSAT. It is just a question of readability and contrast in colors….

Reply: Colors of the maps were modified in order to be easier to observe the frequencies' changes.

Reply to referee #3 first reviews:

Mis en forme : Retrait : Première ligne : 0 cm

We do again apologies about the error that occurred during the first review.

We came back to the first comments and most of them were already answered by responding to the second review previously. Comments about the flow cytometer methodology were asked and we did reply here after.

p.15623
l.11: “with a high spatial resolution (2.2
. . .
”
l.21: “and remote sensing”
l.21: “two to three times better”: is that clear in the text?
p.15624
l.13: “such a proxy”
l.13: “does not”
l.22: define DMSP at first use
l.24: the last properties, thug relevant for the biogeochemical cycles are not directly
linked to the elemental cycles.
p.15625
l.7: I’d suggest: “algorithms applied to remote sensing data”.
l.17: introduce the acronym HPLC
l.21: “SeaWiFS”
l.25: I’d start a new paragraph after “available”.
l.29: “It is critical in understanding
. . .
”: that does not sound correct.
C7226
p.15626
l.16: “in situ data describing phytoplankton
. . .
”
l.18: “with a totally”
l.25: “remotely-sensed”
l.27: “significantly distinct”
Section 2.1: the use of several paragraphs would help in making the description of
methods clearer.
p.15627
l.17: “1-10 cm3 of seawater”
p.15628
l.5: are the 2 trigger levels associated with the 2 photomultipliers?
l.8: “from less concentrated”
l.10-13: this should be explained better.
l.22: “two-dimensional cytograms”: could the authors characterize this in more details?
l.28: PMT: Photo-Multiplier Tube?

Mis en forme : Français (France)

Reply : I thank the reviewer for its interest in the flow cytometer use. I would not add more explanation about the instrument and the data analysis since this section is already important and I would say rarely as complete.

p.15629
l.1-2: sentence not well written
l.6: “pre-determined”: what does this mean?
l.12: “ship’s seawater
. . .
”
l.18: MODIS on-board Aqua I guess
p.15630
C7227
l.6-7: please correct this sentence. Are the data Level-2 or Level-3? (the latter if they
are 4-km data).

l.14: “defined as the depth associated with an observed temperature difference of more
than 0.2C with respect to the surface
. . .
”
l.16: “remotely sensed”
l.21: “aerosol optical thickness” ?
l.22-23: “coastal areas, that are not considered as open waters for remote sensing”:
this sounds awkward; remote sensing (of ocean color) responds to optical properties.
l.24: please develop this point (optical classification) somewhat more. Vantrepotte et
al (2012) distinguished 4 classes. I guess that class memberships were used to select
the conditions of analysis; which criteria were used?
l.25: “which previously rendered
. . .
”: it sounds like that this has changed in the mean-
time. Is it the case? In general, a sentence explaining why PHYSAT is not recom-
mended for turbid waters would be welcome.
p.15631
l.9: “irradiance” or “radiance”? Some more details about how the anomaly is computed
are due here.
l.14: “normality was not applied”: applied is not the proper word here.
l.18: “remotely”
p.15632
l.3: three of four?
l.5: “associated with”

l.5: “samples varying between..”
C7228
l.14: “depths”
l.18: “3 E” ?
l.25: repeating “cluster” each time may not be necessary
p.15633
l.3: “within the Micro2 cluster”: what about the other clusters? Is it related to size?
l.5: “25 pictures collected within 47 counted cells”: what does it mean exactly? Is it
random or related to size?
p.15635
l.3: “remotely”
l.7-9: this further selection is not so clear to me.
p.15636
l.8: “associated with”
l.10: “synthesis”: please explain this further.
l.12: “tongue”?
l.18: “spatial”
p.15637
l.15: I’d remove “which are”
p.15638
l.16: “inter-bloom”: please specify what that refers to.
l.19: “cells cmˆ-3”
l.21: “
. . .
fell when
. . .
”: considering what’s said before, this sounds contradictory.
C7229

Reply : All the remarks are now integrated into the mns.

Mis en forme : Français (France)

Marked-up manuscript version:

High resolution analysis of a North Sea phytoplankton community structure based on *in situ* flow cytometry observations and potential implication for remote sensing.

M. Thyssen[1*], S. Alvain[1], A. Lefèbvre[2], D. Dessailly[1], M. Rijkeboer[4], N. Guiselin[1], V. Creach[3], L.-F. Artigas[1]

[1] {*Université Lille Nord de France* – CNRS UMR 8187 Laboratoire d'Océanologie et de Géosciences, Université du Littoral Côte d'Opale, MREN, 32 Avenue Foch, 62930 Wimereux, France}

[*] {now at : *Aix Marseille Université*, CNRS/INSU, IRD, Mediterranean Institute of Oceanography (MIO), UM 110, *13288 Marseille* }

[2] {IFREMER LER, 150 quai Gambetta, 62200, Boulogne sur Mer, France}

[3] {The Centre for Environment, Fisheries and Aquaculture Science (Cefas), Pakefield Road, NR33 0HT Lowestoft, United Kingdom}

[4] {RWS Centre for Water Management. Laboratory for hydrobiological analysis. Zuiderwagenplein 2, 8224 AD Lelystad, The Netherlands}

*Corresponding author: M. Thyssen (melilotus.thyssen@mio.osupytheas.fr)

Key words: Plankton functional type, automated scanning flow cytometry, PHYSAT, North Sea, mapping.

Mis en forme : Police :16 pt, Gras

Mis en forme : Interligne : Double

Mis en forme : Français (France)

Mis en forme : Retrait : Gauche : 0 cm, Espace Après : 5.95 pt, Interligne : simple

Abstract

Phytoplankton observation in the ocean can be a challenge in oceanography. Accurate estimations of its biomass and dynamics will help to understand ocean ecosystems and refine global climate models. Relevant datasets of phytoplankton defined at a functional level and on a daily and sub meso scale are thus required. In order to achieve this, an automated, high frequency, dedicated scanning flow cytometer (SFC, Cytobuoy, NL), has been developed to cover the entire size range of phytoplankton cells whilst simultaneously taking pictures of the largest of them. This cytometer was directly connected to the water inlet of a pocket Ferry Box during a cruise in the North Sea, 8-12 May 2011 (DYMAPHY project, INTERREG IV A "2 Seas"), in order to identify the phytoplankton community structure of near surface waters (6 m) with a high spatial resolution ~~spatcial~~ basis (2.2 ± 1.8 km). Ten groups of cells, distinguished on the basis of their optical pulse shapes, were described (abundance, size estimate, red fluorescence per unit volume). Abundances varied depending on the hydrological status of the traversed waters, reflecting different stages of the North Sea blooming period. Comparisons between several techniques analyzing ~~chlorophyll~~ chlorophyll *a* and the scanning flow cytometer, using the integrated red fluorescence emitted by each counted cell, showed significant correlations. For the first, time, the community structure observed from the automated flow cytometry dataset was compared with ~~classical~~ PHYSAT reflectance anomalies over a daily scale. The number of matchups observed between the SFC automated high frequency *in situ* sampling and ~~the~~ remote sensing was found to be more than two ~~to three~~ times better than when using traditional water sampling strategies. Significant differences in the phytoplankton community structure within the two days for which matchups were available suggest that it is possible to label PHYSAT anomalies using automated flow cytometry to resolve not only dominant groups, but community structure.

Mis en forme : Police :Italique

1. Introduction

Phytoplankton plays a major role in marine ecosystems as the most important primary producer in the ocean (Field *et al.* 1998). Phytoplankton is involved in the long-term trapping of atmospheric carbon and its role in carbon transfer from the upper ocean layers to deep waters highlight its influence on climate (Boyce *et al.* 2010; Marinov *et al.* 2010). Beyond its role in the carbon cycle, phytoplankton also plays a major role in modifying the biogeochemical properties of water masses by converting most of the inorganic matter into available organic matter (nitrogen, phosphate, silicate, sulfur, iron); and determining the structure of the trophic status of marine environments. Given this importance, it is insufficient to use a single proxy, such as chlorophyll *a* measurements, for quantifying and qualifying phytoplankton over large scales when attempting to understand its role in biogeochemical processes (Colin *et al.* 2004). Such a proxy does not reflect changes in community structure (Hirata *et al.* 2011) and does not yield robust biomass estimations (Kruskopf and Flynn 2006). Yet this classical proxy is frequently used to study the spatial and temporal variability of phytoplankton from both remotely sensed and *in situ* measurements. LeQuéré (LeQuéré *et al.* 2005) pointed out the importance of taking into account the functionality of phytoplankton species when considering the influence of phytoplankton community structure on biogeochemical processes. This functionality concept (i.e. Phytoplankton Functional Types, PFT) is described as set of species sharing similar properties or responses in relation to the main biogeochemical processes such as the N, P, Si, C and S cycles (diazotrophs for N cycle such as Cyanobacteria, ~~DMSP~~ diméthylsulfoniopropionate producers for S cycle such as *Phaeocystis*, silicifiers for Si cycle such as Diatoms, calcifiers for C cycle such as Coccolithophorids, size classes~~, motility, food web structure~~ mainly used for C cycle).

Mis en forme : Police :Non Gras, (Asiatique) Chinois (RPC)

Mis en forme : (Asiatique) Chinois (RPC)

Representative data sets of phytoplankton functional types, size classes and specific chlorophyll *a* concentrations are the subject of active research using high frequency *in situ* dedicated analysis from automated devices such as spectral fluorometers, particle scattering and absorption spectra recording instruments, or automated and remotely controlled scanning flow cytometry (SFC). Among the high frequency *in situ* techniques used to quantify phytoplankton abundance, community structure and dynamics, SFC is the most advanced instrument, counting and recording cell optical properties at the single cell level. This technology has recently been adapted for the analysis of almost all the phytoplankton size classes and focuses on the resolution of phytoplankton community structure dynamics (Dubelaar *et al.* 1999; Olson *et al.* 2003; Sosik *et al.* 2003; Thyssen *et al.* 2008a; Thyssen *et al.* 2008b). In parallel, ~~remote sensed~~ algorithms applied to remote sensing data have been developed which are dedicated to characterizing phytoplankton groups, PFTs or size classes (Sathyendranath *et al.* 2004; Ciotti *et al.* 2006; Nair *et al.* 2008; Aiken *et al.* 2008; Kostadinov *et al.* 2010; Uitz *et al.* 2010; Moisan *et al.* 2012). One of these algorithms, PHYSAT, has provided a description of the dominant phytoplankton functional types (LeQuéré *et al*., 2005) for open waters on a global scale, leading to various studies concerning the PFT variability (Alvain *et al.* 2005; Alvain *et al.* 2013; Masotti *et al.* 2011; Demarcq *et al.* 2011, Navarro *et al.*, 2014). PHYSAT relies on the identification of water-leaving radiance spectra anomalies, empirically associated with the presence of specific phytoplankton groups in the surface water. The anomalies were labeled thanks to the comparison with high pressure liquid chromatography (HPLC) biomarker pigment match ups. To date, six dominant phytoplankton functional groups in open waters (Diatoms, Nanoeucaryotes, *Prochlorococcus*, *Synecochoccus*, *Phaeocystis*-like, Coccolithophorids) have been found to be significantly related to specific water-leaving radiance anomalies from ~~SeaWifs~~ SeaWiFS (Sea-viewing Wide Field-of-view Sensor) sensor measurements at a resolution of 9 km (Alvain *et al.* 2008).

These relationships have been verified by theoretical optical models (Alvain *et al.* 2012). This theoretical study also showed that additional groups or assemblages could be added in the future, once accurate *in situ* observations are available.

Describing the community structure on a regional scale will give better quantification and understanding of the phytoplankton responses to environmental change and consequently, support the modification of theoretical considerations regarding energy fluxes across trophic levels. It is critical ~~in~~ to understanding community structure interactions and particularly when it is necessary to take into account the meso-scale structure in a specific area (D'Ovidio *et al.* 2010), which is the case in areas under the influence of regional physical forcing such as the English Channel and the North Sea. Long-term changes detected in these regions have been shown to impact local ecosystem functioning by inducing, for instance, a shift in the timing of the spring bloom (Wiltshire and Manly 2004, Sharples *et al.* 2009; Vargas *et al.* 2009; Racault *et al.* 2013) or specific migrations of regional (Gomez and Souissi 2007) or dominant phytoplankton groups (Widdicombe *et al.* 2010). In addition, hydrodynamic conditions have been shown to play a strong role in the phytoplankton distribution on a regional scale (Gailhard *et al.* 2002; Leterme *et al.* 2008). It is therefore crucial to develop specific approaches to characterize the phytoplankton community structure (beyond global-scale dominance) and its high frequency variation in time and space. In order to achieve this, large data sets of *in situ* analyses resolving PFT are essential for specific calibration and validation of regional remote sensing algorithms such as PHYSAT. Flow-through surface water properties analysis for remote sensing calibration optimizes the amount of matchups (Werdell et al., 2010; Chase *et al.*, 2013). For the purpose of collecting high resolution *in situ* data describing phytoplankton community structure, automated SFC technology allows samples to be collected at high frequency, resolving hourly and km scales ~~in~~ with a totally automated system. The instrument enables single cell analysis of phytoplankton from 1 to 800 µm and

several mm in length for chain forming cells and automated sampling allows large space and time domains to be covered at a high resolution (Sosik *et al.* 2003; Thyssen *et al.* 2008b; Thyssen *et al.* 2009; Ribalet *et al.* 2010).

Based on this approach, a high frequency study of the phytoplankton community structure in the North Sea was conducted. The *in situ* observations from SFC have been used for the first time and as a first trial to label PHYSAT anomalies detected during the sampling period. Thus, the available dataset makes it possible to distinguish between different water-leaving radiance anomaly signatures in which significantly distinct phytoplankton community structures can be described, rather than just the dominant communities, as it is the case ~~of~~ in previous studies. Our results are an improvement over conventional approaches as they allow the distribution of phytoplankton community structure to be characterized at a high resolution, from both *in situ* and day-to-day water-leaving radiance anomaly maps specific to the study area.

2. Materials and Methods

Samples were collected during the PROTOOL/DYMAPHY-project cruise onboard the RV Cefas Endeavour from the 8 to 12 May 2011 in the south-west region of the North Sea (Figure 1). Automated coupled sampling using a Pocket FerryBox (PFB) and a Cytosense scanning flow cytometer (SFC, Cytobuoy, b.v.) started on the 8 May at 9:00 UTC and ended on the 12 May at 4:00 UTC. Water was continuously collected from a depth of 6 m and entered the PFB at a pressure of 1 bar maximum. Sub-surface discrete samples were collected using Niskin bottles on a rosette and analyzed using a second Cytosense SFC (Stations 4, 6 and 13 were used in this paper, Figure 1).

2.1. Phytoplankton community structure from automated SFC

Phytoplankton abundance and group description were determined by using two Cytosense SFCs (Cytobuoy, b.v.), one was fixed close to the PFB and sampling ~~nearly continuously the flow through~~ the continuous flow of pumped sea ~~water~~ water~~input~~, the second one was used for pictures collection from discrete samples. These instruments are dedicated to phytoplankton single cell recording, enabling cells from 1 µm to 800 µm and several mm in length to be analysed routinely in 1-10 cm^3 of sea water. Each single cell or particle in suspension in the solution ~~will~~ passes through the laser beam thanks to the principle of hydrodynamic focusing. The instrument ~~w~~then~~ill~~ records the resulting optical pulse shapes and count each single particle.

Mis en forme : (Asiatique) Chinois (RPC)

Mis en forme : (Asiatique) Chinois (RPC)

2.1.1. Automation of the ~~flow through~~continuous flow sampling

~~A~~~~For the a~~Automated measurements were run from the ~~flow through~~continuous flow of sea water passing through the PFB.~~,~~ S~~s~~amples for SFC were automatically collected from a 450 cm^3 sampling unit where water from the continuous flow was periodically stabilized. This sampling unit was designed to collect bypass water from the 1 bar PFB inlet. The sampling unit water was replaced within a minute. One of the Cytosenses was directly connected to the sampling unit and two successive analyses with two distinct protocols were scheduled automatically every 10 min.

Mis en forme : Normal, Gauche, Interligne : simple

2.1.2. Flow cytometry analysis

Mis en forme : Titre 3 Car, Anglais (États Unis)

A calibrated peristaltic pump was used to estimate the analysed volumes and send the sample to the SFC optical unit. Suspended particles were then separated using a laminar flow and subsequently crossed a laser beam (Coherent, 488 nm, 20 mV). The instrument recorded the pulse shapes of forward scatter (FWS) and side ward scatter (SWS) signals as well as red, orange and yellow fluorescence (FLR, FLO, FLY respectively) signals for each chain or

Mis en forme : Normal, Gauche, Interligne : simple

single cell. The Cytosense instrument was equipped with two sets of photomultiplier (PMT) tubes (high sensitivity and low sensitivity modes), resolving a wider range of optical signals from small (~<10 µm) to large particles (~<800 µm). Two trigger levels were applied on the high sensitivity PMT to discriminate highly concentrated eukaryotic picophytoplankton and cyanobacteria (trigger level: FLR 10 mV; acquisition time: 180 s; sample flow rate: 4.5 $mm^3.s^{-1}$), from ~~lower~~ less concentrated nano- and microphytoplankton (trigger level: FLR 25 mV, acquisition time: 400 s; sample flow rate: 9 $mm^3.s^{-1}$). Setting the trigger on red fluorescence was preferred to the commonly FWS or SWS triggering as a tradeoff between representative phytoplankton data sets and non-fluorescing particles/noise recording, but this procedure affected the SWS and FWS pulse shapes to some extent. To ensure good control and calibration of the instrument settings, a set of spherical beads with different diameters was analysed daily. This allowed the definition of estimated-size calibration-curves between Total FWS (in arbitrary units) and actual bead size. This set of beads included 1, 6, 20, 45, 90 µm yellow green fluorescence from Polyscience Fluoresbrite microspheres, 10 µm orange fluorescence Invitrogen polystyrene Fluorosphere, and 3 µm 488 nm Cyto-cal™ Alignment standards. To correct for the high refraction index of polystyrene beads that generates an underestimation of cell size, we defined a correcting factor by using 1.5 µm silica beads (Polyscience, Silica microspheres) (Foladori *et al.* 2008). The phytoplankton community was described using several two-dimensional cytograms built with the Cytoclus® software. For each autofluorescing phytoplankton cell analysed, the integrated value of FLR pulse shape (Total red fluorescence TFLR, a.u.) was calculated. For each phytoplankton cluster, the amount of TFLR is reported per unit volume (TFLR.cm^{-3}, a.u..cm^{-3}). The TFLR.cm^{-3} of each resolved phytoplankton cluster was summed (Total TFLR.cm^{-3}) and was used as a proxy for chlorophyll *a* concentration (µg.dm^{-3}). The TFLR signal was corrected from high sensitivity

PMT saturation signal in the case of highly fluorescing cells (> 4000 mV) ~~by using~~thanks to the low sensitivity PMTs that behaved linearly ~~below this value~~ with the high sensitivity PMT, allowing the reconstruction of the high sensitivity signal.~~.~~

Discrete samples were collected during the cruise and analyzed using a second Cytosense SFC equipped with the Image in Flow system. The samples were analysed using settings similar to those of the Cytosense coupled to the PFB. ~~-~~"The amount of pictures was determined before each sample acquisition and pictures were randomly collected within the largest particles until the predetermined number of pictures was reached."~~and pictures were randomly collected for the largest particles until the predetermined number of pictures was reached.~~

2.2. Temperature and Salinity

The PFB (4H-JENA©) was fixed on the wet laboratory bench, close to the Cytosense, in order to share the same water inlet. This instrument recorded temperature and conductivity (from which salinity was computed) from the clean water supplied by the ship's seawater pumping system at a frequency of one sample every minute.

Within the PFB dataset, only data related to automated SFC analyses were selected for plotting temperature – salinity diagrams.

2.3. ~~Chlorophyll~~ Chlorophyll *a*~~a~~

Samples for High Pressure Liquid Chromatography (HPLC) analyses and bench top fluorometry (Turner® fluorometer) were collected randomly within 6 hour periods before or after the supposed on-board Aqua MODIS ~~-~~(Moderate Resolution Imaging Spectroradiometer) sensor passage (12:30 pm UTC) to fulfill classical requirements in terms of *in situ* and remotely sensed matchup criteria. Samples were collected from the outlet of the PFB, filtered

onto GF/F filters and stored directly in a -80°C freezer. The HPLC analyses were run on an Agilent Technologie, 1200 series. Pigments were extracted using 3 cm^3 ethanol containing vitamin E acetate as described by Claustre *et al.* (2004) and adapted by Van Heukelem and Thomas (2001). For bench top fluorometry, the filters were subsequently extracted in 90% acetone. Chlorophyll *a* (chla) concentration was evaluated by fluorometry using a Turner Designs Model 10-AU fluorometer (Yentsch and Menzel 1963). The fluorescence was measured before and after acidification with HCl (Lorenzen 1966). The fluorometer was calibrated using known concentrations of commercially purified chla (Sigma-Aldrich®).

The PFB was equipped with a multiple fixed wavelength spectral fluorometer (AOA fluorometer, bbe©) sampling once every minute to obtain chla values.

MODIS chla values ~~were~~ corresponded to ~~extracted from daily level-2 product~~ Level-3 binned data consisting of the accumulated daily Level-2 data~~determining~~ with a 4.6 km resolution ~~(L3 Binned data)~~.

2.4. Mixed layer depth

Daily water column temperature mapping was obtained from the Forecasting Ocean Assimilation Model 7 km Atlantic Margin model (FOAM AMM7), available at MyOcean data base (http://www.myocean.eu.org/). Model output temperature depths were as follows: 0, 3, 10, 15, 20, 30, 50, 75, 100, 125, 150 m. Average mixed layer depth (MLD) on the 5 sampling days was calculated from daily temperature datasets. MLD was defined as the depth associated with an ~~absolute~~observed temperature difference of more than 0.2 °C ~~from one depth~~with respect to the surface (defined at 10 m, de Boyer Montégut *et al.* 2004).

~~2.5.~~ Matching method between in situ and remotely sensed observations for phytoplankton community structure

Mis en forme : Police :(Par défaut) Arial, Gras

The PHYSAT approach is based on the identification of specific signatures in the water leaving radiance (nLw) spectra measured by an ocean color sensor. It is described in detail by Alvain *et al.* (2005, 2008). Briefly, this empirical method has been first established by using two kinds of simultaneous and coincident measurements: nLw measurements and *in situ* measurements of diagnostic phytoplankton pigments. The presence of a specific phytoplankton group was established based on pigment analysis. In a first step, this approach has allowed to detect four dominant phytoplankton groups identified within the available *in situ* data set, based on the pigment inventories. Four groups were detected first (diatoms, nanoeukaryotes, *Synechococcus* and *Prochlorococcus*) when they are dominant. Note that here, ‘‘dominant’’ has been defined by Alvain *et al.* (2005) as situations in which a given phytoplankton group is a major contributor to the total diagnostic pigments. This represented a limitation in using other potential phytoplankton *in situ* analysis. In a second step, coincident remote sensed radiance anomalies (Ra) spectra between 412 and 555 nm were transformed into specific normalized water-leaving radiance or Ra spectra in order to evidence the second-order variability of the satellite signal. This was done by dividing the actual nLw by a mean nLw model (nLw_{ref}), which depends only on the standard chla.

Then, coincident nLw spectra and *in situ* analysis were used to show that every dominant phytoplankton group sampled during *in situ* sampling is associated with a specific Ra spectrum in terms of shape and amplitude. Based on this, a set of criteria has been defined in order to characterize each group in function of its Ra spectrum, first by minimum and maximum values approach and more recently using neuronal network classification tools (Ben Mustapha *et al.*, 2014). These criteria can be applied to global daily archives to get global maps of the most frequent group of dominant phytoplankton. When no group prevails over the month, the pixels are associated with an ‘‘unidentified’’ phytoplankton group.

Mis en forme : Police :Italique, Anglais (États Unis)

Mis en forme : Police :(Par défaut) Times New Roman, Non Gras, Italique, Anglais (États Unis)

Mis en forme : Police :(Par défaut) Times New Roman, Non Gras, Italique, Anglais (États Unis)

Mis en forme : Police :Italique, Anglais (États Unis)

Mis en forme : Police :Italique, Anglais (États Unis)

Mis en forme : Police :Italique, Anglais (États Unis)

Mis en forme : Police :(Par défaut) Times New Roman, Non Gras, Italique, Anglais (États Unis)

Mis en forme : Anglais (États Unis), Non Surlignage

Mis en forme : Anglais (États Unis), Indice

Mis en forme : Police :(Par défaut) Times New Roman, Non Gras, Italique, Anglais (États Unis)

Mis en forme : Police :(Par défaut) Times New Roman, Non Gras, Italique, Anglais (États Unis)

Mis en forme : Police :Italique, Anglais (États Unis)

In this study, r~~R~~emotely sensed observations were selected on the basis of quality criteria that ensured a high degree of confidence in PHYSAT as described in Alvain *et al.* (2005). Thus, pixels were only considered when clear sky conditions were found and when the aerosol optical thickness, a proxy of the atmospheric correction steps quality, was lower than 0.15. The effects of sediments and/or CDOM were minimized by focusing on phytoplankton dominated waters as defined from the optical typology described in Vantrepotte et al (2012). ~~In addition, as the region of interest included some coastal areas, that are not considered as open waters for remote sensing, we have selected pixels according to their optical properties (Vantrepotte *et al.* 2012). Consequently, this avoided using waters rich in sediment which previously rendered it impossible to use the PHYSAT version.~~ Waters classified as turbid were therefore excluded from the empirical relationship since the PHYSAT method is currently not available for such areas. Waters classified as non-turbid using the same criteria were selected and the PHYSAT algorithm applied. To link coincident *in situ* and remotely sensed observations, a match-up exercise was carried out. Matching points between *in situ* SFC samples (considered as *in situ* data) and 4.6 km resolution MODIS pixels (highest L3 binned resolution) were selected by comparing their concomitant position day after day. When more than one *in situ* SFC sample was found in a MODIS pixel the averaged value of TFLR (a.u..cm^{-3}) for each phytoplankton group was calculated. ~~From the matching points, the PHYSAT method resulted in water leaving irradiance anomalies spectra (Ra) as described in Alvain *et al.* 2008 and 2012.~~

~~2.6.~~2.5. Statistics

Statistics were run under R software (CRAN, http://cran.r-project.org/). Before running correlation and comparison tests on the different *in situ* sensors (for chla and Total TFLR), the Shapiro normality test was run. When data did not follow a normal

Code de champ modifié

distribution~~Normality was not applied~~, a Wilcoxon signed rank test was applied. Correlations between data were defined using Spearman's rank correlation coefficient.

As the PHYSAT approach is based on the link between specific Ra spectra (in terms of shapes and amplitudes) and specific phytoplankton composition, the set of remotely sensed data was separated into distinct groups with similar Ra. The PHYSAT Ra found over the studied area and matching the *in situ* SFC samples was differentiated by applying a k-means clustering partitioning method (tested either around means (Everitt and Hothorn 2006) or around menoids (Kaufman and Rousseeuw 1990)). The appropriate number of clusters was decided with a plot of the within groups sum of squares by number of clusters extracted. A hierarchical clustering was computed to illustrate the k-means clustering method. Within each k-mean cluster, SFC-defined phytoplankton community was described and differences between TFLR.cm^{-3} per phytoplankton group were compared within the different PHYSAT spectra clusters using the Wilcoxon signed rank test.

3. Results

3.1. Temperature, Salinity and Mixed layer depth

The sampling track crossed ~~three~~ four North Sea marine zones: Western Humber, Tyne, Dogger, Eastern Humber and Thames (Fig. 1). The PFB measured temperature associated ~~to~~ with the SFC samples ~~and varied~~ ranged between 8.83 °C and 12.39°C with an average of 10.67 ± 0.72 °C. Minimal temperatures were found in the western Humber area (53-55°N and -1-1°E) and maximal temperatures were found in the Thames area (54-52°N, 2-4°E) (Fig. 2A). Salinity from the PFB ranged between 34.02 and 35.07 with an average value of 34.6 ± 0.26. Highest salinity values were found in the Dogger area above 55°N and in the limit between the Humber and the Thames areas, 53°N. Lowest salinity values were found in the Tyne area around 55°N, -1 °E and in the Thames area (by the Thames plume; Fig. 2B).

The mixed layer depth calculated from the FOAM AMM7 was used to illustrate the physical environment of the traversed water masses. Different mixed layer depth characterized the sampled area, with deeper MLD in the northern part (15 to 30 m) and a shallower MLD in the southern area (~10 m, Fig.1). A tongue of shallow MLD (~10 m) surrounded by deeper MLD (~20 m) crossed the sampling area at ~55°N and ~3°~~W~~E.

3.2. Phytoplankton community from SFC analysis

A total of 247 SFC validated analysed samples were collected during this experiment. Average distance between samples collected with the automated SFC was of 2.2 ± 1.8 km when the system ran continuously. The sampling rate was 25 ± 45 min. Up to 10 phytoplankton clusters were resolved (Fig. 3) based on their optical fingerprints from SFC analysis. The 10 discriminated clusters were labeled as follows: PicoORG ~~cluster~~ (Fig. 3A), PicoRED ~~cluster~~ (Fig. 3A), NanoSWS ~~cluster~~ (Fig. 3B), NanoRED1 ~~cluster~~ (Fig. 3C), NanoRED2 ~~cluster~~ (Fig. 3B and 3C); Micro1 ~~cluster~~ (Fig. 3C and 3D), MicroLowORG (Fig. 3A), NanoORG and MicroORG ~~clusters~~ (Fig. 3D) and ~~a cluster of large cells,~~ Micro2 ~~cluster~~ (Fig 3D). Pictures were randomly collected (between 20 and 60 pictures per sample within ~~the~~ Micro2 ~~cluster~~) and were used to illustrate the most frequently encountered class (Fig. 4). Station 4 (Fig. 4A) sampled at 12 m, showed mostly a mixture of dinoflagellate-like cells (25 pictures collected within 47 counted cells). Station 6 (Fig. 4B) sampled at 7 m, showed pictures composed mainly of diatoms (*Thalassiosira* and *Chaetoceros*, 11 images collected among 28 counted cells). Station 13 (Fig. 4C) sampled at 7 m, gave a mixture of diatoms and dinoflagellates (58 pictures shot among the 99 counted cells corresponding to the Micro2 cluster: 5 *Chaetoceros*, 30 *Rhizosolenia*, 10 Dinoflagellates, one flagellate and several unidentified cells).

808 Cell abundance, average cell size and TLFR.cm^{-3} for each cluster are illustrated on
809 Figures 5, 6 and 7 respectively. Average abundance and sizes of each cluster are addressed in
810 Table 1. PicoRED cells were on average, the most abundant in the studied area (Fig. 5B and
811 Table 1) followed by NanoRED2, PicoORG, NanoRED1 and Micro1 (Fig. 5F, 5A, 5C and 5G
812 respectively, Table 1). The other cluster's abundances were below 1.10^{2} cells.cm^{-3} on average
813 (Fig. 5D, E, H, I, J; Table 1). PicoORG cells were the smallest estimated (Fig. 6A, Table 1),
814 while the largest estimated were MicroORG, MicroLowORG and Micro2 cells (Fig. 6H, 6I
815 and 6J respectively, Table 1).
816 The western Humber zone (Fig.1) was marked by the highest abundances of PicoRED,
817 PicoORG, MicroORG, MicroLowORG and Micro1 (Fig. 5B, 5A, 5H, 5I and 5G). The eastern
818 part of the Humber zone (Fig.1) was marked by the highest abundances of NanoRED1 and
819 Micro1 (as for the western part) (Fig. 5C, 5G). High values of PicoRED were also observed in
820 this part of the Humber zone. The Tyne zone (Fig.1) had the highest abundance of NanoORG
821 and Micro2 clusters (Fig. 5D, 5J), and the lowest abundance of PicoRED and NanoSWS.
822 High abundance values of MicroORG were also observed (Fig. 5H). The size of the
823 NanoSWS and the NanoRED2 were the greatest in this zone (Fig. 6E, 6F). The Dogger zone
824 (Fig.1) was dominated in terms of abundance by the PicoRED and the PicoORG, where the
825 sizes were the smallest (Fig. 6B and 6A) but did not show the highest abundance values. The
826 cell sizes of Micro1 were the greatest in this zone (Fig. 6G). Observations in the Thames zone
827 (Fig.1) produced the maximal abundance of NanoSWS and NanoRED2 (Fig. 6E, 6F). Sizes
828 were the greatest for PicoORG, NanoRED1 and NanoSWS (together with the Tyne zone; Fig.
829 6A, 6C, 6E). TFLR follows similar trends to abundance (Fig. 7).
830
831 **3.3. Comparison between scanning flow cytometry, Total Red Fluorescence**
832 **and chlorophyll *a* analysis**

Mis en forme : Police :(Par défaut) Arial, Gras, Italique, Anglais (États Unis)

Several bench top and *in situ* instruments, i.e. HPLC, Turner fluorometer and the PFB AOA fluorometer, were used to give either exact and/or proxy values of chla. Similarly to temperature and salinity, the PFB AOA fluorometer samples were selected to match SFC samples. Overall values of chla originating from these instruments were superimposed to the Total TFLR.cm^{-3} (by summing up the TFLR.cm^{-3} values of the observed cluster) and the MODIS chla values matching the points on Figure 8. HPLC values varied between 0.21 and 7.58 µg.dm^{-3} with an average of 1.57 ± 2.01 µg.dm^{-3}. Turner fluorometer values varied between 0.41 and 2.31 with an average of 1.24 ± 0.7 µg.dm^{-3}. AOA fluorometer values varied between 0.73 and 28.53 µg.dm^{-3} with an average of 4.44 ± 5.54 µg.dm^{-3}. The Total TFLR.cm^{-3} from SFC, normalized with 3 µm bead red fluorescence varied between 5011 and 399200 a.u..cm^{-3} with an average value of 64394.5 ± 67488.4 a.u..cm^{-3}. The Shapiro normality test showed non normality for each of the variables so a Wilcox test was run between techniques involving similar units. HPLC and Turner chla concentrations were significantly not different ($n=9$, $p=0.65$) and the correlation was significant (Spearman, $r=0.98$, Table 2). The absolute values from both techniques were significantly different from the AOA fluorometer values ($n=9$, $p<0.001$ for both) but were significantly correlated (Spearman, $r=0.86$ and $r=0.82$ for HPLC and Turner fluorometer respectively, Table 2). The SFC Total TFLR (a.u..cm^{-3}) summing up the TFLR of all the phytoplankton groups was used for comparison with other chla determinations. Correlations with the AOA fluorometer, the HPLC and the Turner fluorometer results were all significant as shown in Table 2.

3.4. PHYSAT anomalies and SFC phytoplankton community composition, extrapolation to the non-turbid classified waters in the North Sea

Considering our database of coincident SFC *in situ* and MODIS remotely sensed observations, a total of 56 matching points were identified, from which only 38 points corresponded to non-turbid classified waters. Matching points between *in situ* sampling and remote sensing pixels for the purpose of the PHYSAT empirical calibration were selected in the daytime period 6 - 18 h. Additional samples collected out of this period results in the loss of~~, the limit of the~~ correlation significance between MODIS chla and the AOA fluorometer chla within the SFC dataset (r=0.49, p=0.06, n=15, Spearman rank test), leaving 15 SFC matching points (Fig. 1 and Fig. 8). The chla values found in the matching points were lower than 0.5 µg.dm^{-3} (Fig. 8).

PHYSAT radiance anomalies (Ra) were calculated based on the 2005 method (Alvain *et al.*, 2005) and the average signal was recalculated to fit the sampling area. The Ra were separated into two distinct anomalies using the within sum of square minimization (Fig. 9A) and illustrated on a dendrogram (Fig. 9B). These two distinct types of anomalies in terms of shape and amplitude are illustrated in Figure 9C and 9D and the anomaly characteristics are summarized on Table 3. The first anomaly set (N1, Table 3) was composed of 5 spectra that had overall higher values than the second anomaly set (N2, Table 3), composed of the other 10 spectra. The corresponding SFC cluster proportion of TFLR.cm^{-3} to the overall Total TFLR.cm^{-3} found within the two anomalies are illustrated in Figures 10 A and B. Similarly, the relative difference of each phytoplankton cluster's TFLR.cm^{-3} within the two anomalies to its overall TFLR.cm^{-3} median value are illustrated in Figures 10 C and D. Considering our previous analyses, N1 and N2 community structures were dominated by NanoRED2 TFLR.cm^{-3} (Fig. 10A and 10B). Regarding each distinct cluster relative difference to its overall median value, samples corresponding to N1 anomalies had significantly higher NanoRED1 TFLR.cm^{-3}, higher NanoORG TFLR.cm^{-3} and higher MicroORG TFLR.cm^{-3};

while the samples corresponding to N2 anomalies had only higher PicoRED TFLR.cm^{-3} (Wilcox rank test, N1, n=5; N2, n=10, Fig. 10C and 10D). Temperature, salinity, MODIS chla and SFC Total TFLR.cm^{-3} found in each *in situ* sample corresponding to both sets of anomalies are illustrated in Fig. 11. Samples found in the N1 pixels were significantly warmer (11.3 ± 0.32°C in N1 and 10.94 ± 0.23°C in N2, $p<0.1$, Wilcox rank test, Fig. 11A), not significantly different in terms of salinity, although N1 waters were less salty (Fig. 11B), significantly richer in chla ($p<0.01$, Wilcox rank test, Fig. 11C), but not significantly different in Total TFLR.cm^{-3} values (Fig. 11D).

Considering the specificity of each set of Ra in terms of phytoplankton and environmental conditions, it's interesting to map their frequency of detection in our area of interest. A pixel is associated ~~to~~ with an anomaly when the Ra values at each wavelength fulfilled the criteria of Table 3. The frequencies of occurrence over the sampling period based on a composite ~~synthesis~~ overlapping the sampling period are illustrated in Fig. 12A and 12B. Pixels corresponding to N1 anomaly were mostly found in the 54-56°N area (Dogger and German, Fig. 1), following the edge between the shallow MLD tongue and the deepest MLD zones (Fig. 1), but also near the Northern Scottish coast (Forth, Forties and Cromarty, Fig. 12A), where MLD was shallow (Fig. 1). The N2 anomaly pixels were mostly found in the Forties, Fisher and German area, on much smaller surfaces (Fig. 12B).

4. Discussion

~~The automated SFC used during this study resolves the spacial/temporal issue by its high frequency sampling, reaching sub-mesoscale distribution and diel changes in abundances. However, w~~Water mass dynamics generates patchiness which modifies phytoplankton community structure and makes it difficult to follow a population over time

and at a basin scale. In this context, the hourly observation of phytoplankton at the single cell and the community level and ~~the~~its daily spatial structure resolution from ~~-~~extrapolation ~~of the community structure~~ using PFT ~~daily~~ remote sensing mapping can help to follow spatial distribution of phytoplankton communities. The improvement of PFT mapping, i.e. from dominant groups to the community structure resolution, is one of the ideas generated in this paper. This paper shows for the first time that SFC datasets can be used for labeling PHYSAT anomalies at the daily scale. The ~~SCF~~ SFC is a powerful automated system aimed to be implemented in several vessels of opportunity and monitoring programs for future PHYSAT anomalies identification at the daily scale and at the community structure level. A recent publication that enables the classification of a large range of anomaly spectra (Ben Mustapha *et al*., 2014) should help to make this easier. Thus, the knowledge and the tools are available, which augurs well for understanding phytoplankton heterogeneity and variability over high ~~frequency~~ resolution spatio-temporal scales.

Indeed, resolving phytoplankton community structure over the sub meso scale and hourly scale is a good way to understand the influence of environmental short scale events (Thyssen et al., 2008a; Lomas *et al.* 2009), seasonal (or not) succession schemes, resilience capacities of the community after environmental changes and impacts on the specific growth rates (Sosik *et al.* 2003, Dugenne et al., 2014). Resolving the community structure and the causes of variations at several temporal and spatial scales has great importance in further understanding the phytoplankton functional role in biogeochemical processes. This scale information is currently lacking for the global integration of phytoplankton in biogeochemical models, mainly due to the lack of adequate technology which ~~are~~ is needed to integrate the different levels of complexity linked to phytoplankton community structure.

Phytoplankton community description

Mis en forme : Retrait : Première ligne : 0 cm

Mis en forme : Police :Gras

Mis en forme : Retrait : Première ligne : 0 cm

Phytoplankton community structure from automated SFC is described through clusters of analyzed particles sharing similar optical properties. Thus cluster identification at the species level is speculative and, as any cytometric optical signature, it needs a sorting and genetic or microscopic analysis to be resolved at the taxonomic~~al~~ level. This deep level of phytoplankton diversity resolution requirement is ~~although~~ not needed in biogeochemical processes studies in which functionality is preferred to taxonomy (LeQuéré et al., 2005). In this context, most of the optical clusters could be described at the plankton functional type level because of some singular similarities combining abundance, size, pigments and structure proxies obtained from optical SFC variables (Chisholm *et al.* 1988; Veldhuis and Kraay 2000; Rutten *et al.* 2005; Zubkov and Burkill 2006). The Cytobuoy instrument used in this study was developed to identify phytoplankton cells from picophytoplankton up to large microphytoplankton with complex shapes, even those forming chains. Indeed, the volume analyzed was close to 3 cm^3, giving accurate counts of clusters with abundances as low as 30 $cells.cm^{-3}$ (100 cells counted), under which, coefficient of variation exceeds 10% (Thyssen et al., 2008a). Such low abundances were found for some of the clusters identified in this study (NanoORG, MicroORG and Micro2 clusters for which the median abundance value was close to 30 $cells.cm^{-3}$), in agreement with concentrations observed in previous studies for the possibly~~e~~ related ~~taxonomical~~ phytoplankton genus, as discussed below, i.e. cryptophytes (Buma *et al.* 1992), diatoms and dinoflagellates (Leterme *et al.* 2006). Previous comparisons between bench top flow cytometry and remote sensing (Zubkov and Quartly, 2003) could technically not include the entire size range of nano-microphytoplankton. The Cytobuoy SFC resolves cells up to 800 µm in theory, but this depends on the counted cells in the volume sampled (which is approximately ten times more than classical flow cytometry). However, the largest part of phytoplankton production in the North Sea is driven by cells < 20 µm (Nielsen *et al.* 1993), and we can consider this size class to be correctly counted with the SFC.

Mis en forme : Retrait : Première ligne : 1.25 cm

Furthermore, significance between the sum of each cluster's TFLR (Total TFLR.cm^{-3}) and bulk chlorophyll measurements (Table 2 and Fig. 7) confirms the power of SFC for phytoplankton community resolution.~~.~~

PicoORG cells could be labeled *Synechococcus* (Waterbury *et al.* 1979*;* Li1994) based on their phycoerythrin pigment fluorescence (Fig. 3A), their size estimated between 0.8 and 1.2 µm (Fig. 6A) and their abundances around 10^{2} - 10^{4} cells.cm^{-3} (Fig. 5A). PicoRED cells could be autotrophic eukaryotic picoplankton, as their cell size varied between 1-3 µm (Fig. 6B) and contained chla as their main pigment. Thus, PicoORG and PicoRED clusters contained the smallest cells found above the so called non-fluorescing/electronical noise background of this instrument (Fig. 3A and 3B). As *Prochloroccocus* is expected to be absent in these waters, we can conclude that the cytometer observed most of the phytoplankton size classes when sufficiently concentrated in the analysed volume. NanoRED1 cells exhibited abundance and sizes close to those of *Phaeocystis* haploid flagellate cells (3-6 µm, Fig. 6C, Rousseau *et al.* 2007 and references therein). Their presence, found mostly in the Humber (Fig. 5C), suggests that this area corresponded to a period between the inter-bloom (haploid stage, life stage persisting between two blooms of diploid colonial cells) and the start of the *Phaeocystis* bloom (Rousseau et al., 2007). Similarly, NanoRED2 could be referred to as *Phaeocystis* diploid flagellates or free colonial cells, based on their size and abundance (4-8 µm and 0-50.10^{3} cells.cm^{3} (Fig. 6F and 5F respectively), Rousseau et al., 2007). Their maximal abundance was found in the southern North Sea Thames area. ~~This abundance fell~~ Their presence suggested an area of ~~when~~ *Phaeocystis* colonial blooming stage ~~was blooming~~ (Guiselin 2010).

MicroORG cells, whose abundance and size are close to those of some large cryptophytes cells, were found in the same areas as NanoORG cells (Fig. 5H and 5D respectively), which are related to smaller *Cryptophyceae* cells. MicroLowORG cells with

sizes close to that of MicroORG cells and although low in concentration, emitted orange fluorescence and could represent cells with little phycoerythrin content. NanoSWS cluster was composed of high SWS ~~diffusing~~ scattering cells that are consistent with the signature of *Coccolithophorideae* cells (van Bleijswijk *et al.* 1994; Burkill et al., 2002). The observed abundances did fit with the low *Coccolithophorideae* concentrations observed in the southern North Sea (Houghton, 1991).

The Micro1 cluster could correspond to small nanoplanktonic diatom cells (~10-30 µm, Fig. 6G). Regarding the size range, this cluster could represent several species. They were mainly found within the Humber area. The Micro2 cluster was mostly composed of large diatoms (*Rhizosolenia*, *Chaetoceros*) and dinoflagellates (Fig. 4) within the size range of 40 - 100 µm (Fig. 6J) as observed in the pictures (Fig. 4). The presence of these groups illustrates the boundary between the end of the diatom bloom and the development of a dinoflagellate bloom, from which it could be possible to make a link with the *Dinophysis norvegica* and *Alexandrium* early summer bloom, observed in the Tyne region by Dodge (Dodge 1977). This is in agreement with the stratification observed within the Thames zone (Fig.1).

Phytoplankton community structure at the North Sea basin scale

Mis en forme : Police :Gras

Mis en forme : Retrait : Première ligne : 0 cm

The data sets from the spatial (km) and the temporal (hourly) scales for phytoplankton community structure based on single cell optical properties are important for validating the methods ~~for~~ describing phytoplankton community structure from space. Ocean algorithms need specific information on water properties and phytoplankton structure and are dependent on validation from *in situ* observations, always complex to collect and limited by sky condition criteria. The PHYSAT method was built on an empirical relationship between dominant phytoplankton functional types from *in situ* HPLC analysis and Ra. The method was thus limited to dominance cases only as HPLC analysis can't give us more information.

1006 The remote sensing synoptic extrapolation concerning phytoplankton community structure
1007 remains to be established and in spite of a theoretical validation (Alvain *et al.*, 2012), still
1008 depends on important *in situ* data point collection in order to build robust empirical
1009 relationships. In this study, the combination of phytoplankton high frequency analysis from an
1010 automated SFC with the PHYSAT method proved to be an excellent calibration by giving an
1011 unprecedented amount of matching points for only two significant sampling days (number of
1012 analyzed samples for non-turbid waters matching MODIS pixels: 38, number of used samples
1013 between 6 and 18h: 15, corresponding to 39.5 % profitability), compared to the 14% matching
1014 points from the GeP&CO dataset (Alvain *et al.*, 2005).

1015 The combination of SFC and PHYSAT has shown that a first set of specific anomalies
1016 (N1) can be associated with NanoRED1, NanoORG and MicroORG, which contributed more
1017 to the Total TFLR.cm^{-3} (a proxy of chla, Fig. 7, Table 2) than in the second set of anomaly
1018 (N2), in which PicoRED cells contributed significantly more to the Total TFLR.cm^{-3}, but also,
1019 where Micro1 contribution to Total TFLR.cm^{-3} was above its overall median value observed
1020 along the matching points (Fig. 10D). Spatial successions between diatoms (as could be found
1021 in the NanoRED1 and Micro1 clusters) and cryptophytes (corresponding to the NanoORG
1022 and MicroORG specific signatures) revealed differences in stratification, lower salinity and
1023 shallower MLD (Moline *et al.* 2004; Mendes *et al.* 2013). Indeed, the N1 anomaly
1024 corresponds to areas of low MLD (Fig. 1) following the main North Sea current from the
1025 south west to the north east (Holligan *et al.* 1989), surrounding the Dogger bank. This
1026 anomaly was also found on the north-western part of the northern North Sea, following the
1027 Scottish coastal water current with a shallow MLD (Fig 1 and Fig 11A). The N2 anomaly was
1028 observed with the deeper MLD of the Forties, Fisher and German areas (Fig. 1 and 11B).
1029 These N2 areas corresponded to a phytoplankton community still blooming while the N1
1030 anomaly areas might be at a stage of late blooming, in which conditions fit cryptophyceae

Mis en forme : Normal, Gauche, Retrait : Première ligne : 0 cm, Interligne : simple

development and grazing (cells of *Myrionecta rubra* were observed when using the Image in Flow, not shown). These organisms were found dominating the areas surrounding the Dogger bank from observations and counts carried out by Nielsen *et al.* (1993) during the same period.

In conclusion, our study of phytoplankton community structure distribution resolved at the sub mesoscale evidenced the importance of the North Sea hydrological context. Significant differences between the two sets of anomalies ~~communities~~ observed during the sampling period are mainly due to cryptophyte like cells and ~~bellow~~ pico-nanophytoplankton size class cells. This daily scale resolution thanks to high resolution techniques meeting single cell and remote technologies will help in understanding the role of circulation and hydrological properties of the water masses on the phytoplankton composition, succession schema, spreading and bloom triggering and collapsing.

~~In conclusion, the use of automated SFC Cytosense technology is an area of great interest when coupled with remote sensing algorithms in the study of surface phytoplankton distribution. Further advances in understanding the link between the phytoplankton community composition and distribution, with radiance anomalies are expected from improvements in analyzing larger volumes by automated SFC and by substantially increasing the number of coincidences between remote sensing and *in situ* observations.~~

Acknowledgement

This study was funded by the DYMPAHY (Development of a DYnamic observation system for the assessment of MArine water quality, based on PHYtoplankton analysis) INTERREG IVA “2 Mers Seas Zeeën” European cross-border project, co-funded by the European Regional Development Fund (ERDF) and French (ULCO-CNRS-UL1), English (Cefas) and Dutch (RWS) partners. We thank the captain and crew of the RV Cefas

"Endeavour", as well as Anne-Hélène Rêve for chlorophyll *a* bench top analysis. We also thank Dr. Rodney Forster for his invitation onboard the ship during the EU FP7 PROTOOL (Automated Tools to Measure Primary Productivity in European Seas) cruise. We are also grateful to our funding sources, the CNRS, the CNES-TOSCA/PHYTOCOT project. The authors thank NASA/GSFC/DAAC for providing access to daily L3 MODIS binned products.

References

Aiken, J., N. J. Hardman-Mountford, R. Barlow, J. Fishwick, T. Hirata and T. Smyth (2008). Functional links between bioenergetics and bio-optical traits of phytoplankton taxonomic groups: an overarching hypothesis with applications for ocean colour remote sensing. Journal of Plankton Research 30(2): 165-181.

Alvain, S., C. Le Quéré, L. Bopp, M. F. Racault, G. Beaugrand, D. Dessailly and E. Buitenhuis (2013). Rapid climatic driven shifts of diatoms at high latitudes. Remote Sensing of Environment 132: 195-201.

Alvain, S., H. Loisel and D. Dessailly (2012). Theoretical analysis of ocean color radiances anomalies and implications for phytoplankton groups detection in case 1 waters. Optics Express 20(2): 1070-1083.

Alvain, S., C. Moulin, Y. Dandonneau and F. M. Bréon (2005).Remote sensing of phytoplankton groups in case 1 waters from global SeaWiFS imagery. Deep Sea Research Part I: Oceanographic Research Papers 52(11): 1989-2004.

Alvain, S., C. Moulin, Y. Dandonneau and H. Loisel (2008). Seasonal distribution and succession of dominant phytoplankton groups in the global ocean : A satellite view. Global Biogeochemical Cycles 22: GB3001.

Ben Mustapha Z., Alvain S., Jamet C, Loisel H. and D. Dessailly. Automatic classification of water leaving radiance anomalies from global SeaWifS imagery : Application to the detection of phytoplankton groups in open ocean waters. Remote Sensing of Environment RSE-08794, 2014.

Boyce, D. G., M. R. Lewis and B. Worm (2010).Global phytoplankton decline over the past century. Nature 466(7306): 591-596.

Buma, A. G. J., W. W. C. Gieskes and H. A. Thomsen (1992).Abundance of cryptophyceae and chlorophyll b-containing organisms in the Weddell-Scotia Confluence area in the spring of 1988. Polar Biology 12(1): 43-52.

Burkill, P.H., Archer, S.D., Robinson, C., Nightingale, P.D., Groom, S.B., Tarran, G.A., and Zubkov, M.V. 2002. Dimethyl sulphide biogeochemistry within a coccolithophore bloom (DISCO): an overview. Deep-Sea Res. II, 49: 2863–2885

Chase, A., Boss, E., Zaneveld, R., Bricaud, A., Claustre, H., Ras, J., Dall'Olmo, G. and T.K.

Mis en forme : Police :Italique

Mis en forme : Interligne : Double

Mis en forme : (Asiatique) Chinois (RPC), (Autres) Français (France)

Mis en forme : (Asiatique) Chinois (RPC), (Autres) Français (France)

Westberry, (2013). Decomposition of in situ particulate absorption spectra. Methods in Oceanography, 7: 110-124.

Chisholm, S. W., R. J. Olson and C. M. Yentsch (1988). Flow cytometry in oceanography: Status and prospects. Eos, Transactions American Geophysical Union 69(18): 562-572.

Ciotti, A. and A. Bricaud (2006). Retrievals of a size parameter for phytoplankton and spectral light absorption by Colored Detrital Matter from water-leaving radiances at SeaWiFS channels in a continental shelf region off Brazil. Limnol. Oceanogr. Methods 4: 237–253.

Claustre, H., S. B. Hooker, L. Van Heukelem, J.-F.Berthon, R. Barlow, J. Ras, H. Sessions, C. Targa, C. S. Thomas, D. van der Linde and J.-C. Marty (2004). An intercomparison of HPLC phytoplankton pigment methods using in situ samples: application to remote sensing and database activities. Marine Chemistry 85(1-2): 41-61.

Colin, P., I. , C. Le Quéré, E. Buitenhuis, J. House, C. Klaas and W. Knorr (2004). Biosphere dynamics: challenges for Earth system models. The State of the Planet: Frontiers and Challenges,. C.J. Hawkesworth and R.S.J. Sparks (eds), American Geophysical Union

D'Ovidio, F., S. De Monte, S. Alvain, Y. Dandonneau and M. Levy (2010). Fluides dynamical niches of phytoplankton types. PNAS.

de Boyer Montégut, C., G. Madec, A. S. Fischer, A. Lazar and D. Iudicone (2004). Mixed layer depth over the global ocean: An examination of profile data and a profile-based climatology. Journal of Geophysical Research: Oceans 109(C12): C12003.

Demarcq, H., G. Reygondeau, S. Alvain and V. Vantrepotte (2011).Monitoring marine phytoplankton seasonality from space. Remote Sensing of Environment 117: 211-222.

Dodge, J. D. (1977). The early summer bloom of dinoflagellates in the North Sea, with special reference to 1971. Marine Biology 40: 327-336.

Dubelaar, B. J., P. Gerritzen, A. E. R. Beeker, R. Jonker and K. Tangen (1999). Design and first results of Cytobuoy: a wireless flow cytometer for in situ analysis of marine and fresh waters. Cytometry 37: 247-254.

Dugenne, M., M. Thyssen, D. Nerini, C. Mante, J.-C. Poggiale, N. Garcia, F. Garcia and G. J. Gregori (2014). Consequence of a sudden wind event on the dynamics of a coastal phytoplankton community: an insight into specific population growth rates using a single cell high frequency approach. Frontiers in Microbiology 5: 485. doi: 10.3389/fmicb.2014.00485

Everitt, B. S. and T. Hothorn (2006).A Handbook of Statistical Analyses Using R, Chapman & Hall.

Field, C. B., M. J. Behrenfeld, J. T. Randerson and P. G. Falkowski (1998). Primary production of the biosphere: integrating terrestrial and oceanic components. Science 281: 237-240.

Foladori, P., A. Quaranta and G. Ziglio (2008). Use of silica microspheres having refractive index similar to bacteria for conversion of flow cytometric forward light scatter into biovolume. Water Research 42(14): 3757-3766.

Gailhard, I., P. Gros, J. P. Durbec, B. Beliaeff, C. Belin, E. Nézan and P. Lassus (2002). Variability patterns of microphytoplankton communities along the French coasts. Marine Ecology Progress Series 242: 39-50.

Mis en forme : (Asiatique) Chinois (RPC)

Mis en forme : (Asiatique) Chinois (RPC), (Autres) Français (France)

1136 Gomez, F. and S. Souissi (2007). Unusual diatoms linked to climatic events in the
1137 northeastern English Channel. Journal of Sea Research 58: 283-290.

1138 Guiselin, N. (2010). Etude de la dynamique des communautés phytoplanctoniques par
1139 microscopie et cytométrie en flux, en eaux côtières de la Manche orientale. ULCO-
1140 MREN. Doctorate (Ph.D.) Thesis in Biological Oceanology, University of Littoral Côte
1141 d'Opale (ULCO), 190 pp.

1142 Hirata, T., N. J. Hardman-Mountford, R. J. W. Brewin, J. Aiken, R. Barlow, K. Suzuki, T.
1143 Isada, E. Howell, T. Hashioka, M. Noguchi-Aita and Y. Yamanaka (2011). Synoptic
1144 relationships between surface Chlorophyll-a and diagnostic pigments specific to
1145 phytoplankton functional types. Biogeosciences 8(2): 311-327.

1146 Holligan, P. M., T. Aarup and S. B. Groom (1989). The North Sea: Satellite colour atlas.
1147 Continental Shelf Research 9(8): 667-765.

1148 Houghton, S. D. (1991). Coccolith sedimentation and transport in the North Sea. Marine
1149 Geology 99(1-2): 267-274.

1150 Kaufman, L. and P. J. Rousseeuw (1990). Finding Groups in Data: An Introduction to Cluster
1151 Analysis, Wiley-Interscience.

1152 Kostadinov, T. S., Siegel, D. A., and Maritorena, S. (2009). Retrieval of the particle size
1153 distribution from satellite ocean color observations, J. Geophys. Res., 114, C09015,
1154 doi:10.1029/2009JC005303.

1155 Kruskopf, M. and K. J. Flynn (2006). Chlorophyll content and fluorescence responses cannot
1156 be used to gauge phytoplankton biomass, nutrient status or growth rate. New
1157 Phytologist 169: 525-536.

1158 LeQuéré, C. L., S. P. Harrison, I. Colin Prentice, E. T. Buitenhuis, O. Aumont, L. Bopp, H.
1159 Claustre, L. Cotrim Da Cunha, R. Geider, X. Giraud, C. Klaas, K. E. Kohfeld, L.
1160 Legendre, M. Manizza, T. Platt, R. B. Rivkin, S. Sathyendranath, J. Uitz, A. J. Watson
1161 and D. Wolf-Gladrow (2005). Ecosystem dynamics based on plankton functional types
1162 for global ocean biogeochemistry models. Global Change Biology 11(11): 2016-2040.

1163 Leterme, S., R. D. Pingree, M. D. Skogen, L. Seuront, P. C. Reid and M. J. Attrill (2008).
1164 Decadal fluctuations in North Atlantinc water inflow in the North Sea between 1958-
1165 2003: impact on temperature and phytoplankton populations. Oceanologia 50(1): 59-72.

1166 Leterme, S. C., L. Seuront and M. Edwards (2006).Differential contribution of diatoms and
1167 dinoflagellates to phytoplankton biomass in the NE Atlantic Ocean and the North Sea.
1168 Marine Ecology-progress Series 312: 57-65.

1169 Li, W. K. W. (1994). Primary production of prochlorophytes, cyanobacteria and eukaryotic
1170 ultraphyto-plankton: Measurements from flow cytometric sorting. Limnology and
1171 Oceanography 39: 169–175.

1172 Lomas, M. W., N. Roberts, F. Lipschultz, J. W. Krause, D. M. Nelson and N. R. Bates (2009).
1173 Biogeochemical responses to late-winter storms in the Sargasso Sea. IV. Rapid
1174 succession of major phytoplankton groups. Deep Sea Research I 56: 892-909.

1175 Lorenzen, C. J. (1966). A method for the continuous measurement of in vivo chlorophyll
1176 concentration. Deep Sea Research I 13: 223-227.

1177 Marinov, I., S. C. Doney and I. D. Lima (2010). Response of ocean phytoplankton community
1178 structure to climate change over the 21st century: partitioning the effects of nutrients,
1179 temperature and light. Biogeosciences Discuss. 7(3): 4565-4606.

Masotti, I., C. Moulin, S. Alvain, L. Bopp and D. Antoine (2011). Large scale shifts in phytoplankton groups in the Equatorial Pacific during ENSO cycles. Biogeosciences 8: 539-550.

Mendes, C. R. B., V. M. Tavano, M. C. Leal, M. S. Souza, V. Brotas and C. A. E. Garcia (2013). Shifts in the dominance between diatoms and cryptophytes during three late summers in the Bransfield Strait (Antarctic Peninsula). Polar Biology 36(4): 537-547.

Moisan, T. A. H., S. Sathyendranath and H. A. Bouman (2012). Ocean Color Remote Sensing of Phytoplankton Functional Types, ISBN: 978-953-51-0313-4, InTech.

Moline, M. A., H. Claustre, T. K. Frazer, O. Schofield and M. Vernet (2004).Alteration of the food web along the Antarctic Peninsula in response to a regional warming trend. Global Change Biology 10(12): 1973-1980.Navarro, G., S. Alvain, V. Vantrepotte and I. E. Huertas (2014). Identification of dominant phytoplankton functional types in the Mediterranean Sea based on a regionalized remote sensing approach. Remote Sensing of Environment 152(0): 557-575.

Navarro, G., S. Alvain, V. Vantrepotte and I. E. Huertas (2014). Identification of dominant phytoplankton functional types in the Mediterranean Sea based on a regionalized remote sensing approach. Remote Sensing of Environment 152(0): 557-575.

Nair, A., S. Sathyendranath, T. Platt, J. Morales, V. Stuart, M.-H, N. Forget, E. Devred and H. Bouman (2008). Remote sensing of phytoplankton functional types. Remote Sensing of Environment 112(8): 3366-3375.

Nielsen, T. G., B. Lokkegaard, K. Richardson, F. Pedersen and L. Hansen (1993).Structure of plankton communities in the Dogger Bank area (North Sea) during a stratified situation. Marine Ecology Progress Series 95: 115:131.

Olson, R. J., A. Shalapyonok and H. M. Sosik (2003). An automated flow cytometer for analyzing pico- and nanophytoplankton=FlowCytobot. Deep Sea Research Part I 50: 301-315.

Racault, M. F., C. Le Quéré, E. Buitenhuis, S. Sathyendranath and T. Platt (2013). Phytoplankton phenology in the global ocean. Ecological Indicators 14(1): 152-163.

Ribalet, F., A. Marchetti, K. A. Hubbard, K. Brown, C. A. Durkin, R. Morales, M. Robert, J. E. Swalwell, P. D. Tortell and E. V. Armbrust (2010). Unveiling a phytoplankton hotspot at a narrow boundary between coastal and offshore waters. Proceedings of the National Academy of Sciences 107(38): 16571-16576.

Rousseau, V., M.-J.Chrétiennot-Dinet, A. Jacobsen, P. Verity and S. Whipple (2007). The life cycle of Phaeocystis: state of knowledge and presumptive role in ecology. Biogeochemistry 83(1-3): 29-47.

Rutten, T. P. A., B. Sandee and A. R. T. Hofman (2005). Phytoplankton monitoring by high performance flow cytometry: A successful approach? Cytometry Part A 64A(1): 16-26.

Sharples, J., C. M. Moore, A. E. Hickman, P. M. Holligan, J. F. Tweddle, M. R. Palmer and J. H. Simpson (2009). Internal tidal mixing as a control on continental margin ecosystems. Geophysical Research Letters 36(23): L23603.

Sathyendranath, S., W. Louisa, D. Emmanuel, P. Trevor, C. Carla and M. Heidi (2004). Discrimination of diatoms from other phytoplankton using ocean-colour data. Marine Ecology Progress Series 272: 59-68.

Sosik, H. M., R. J. Olson, M. G. Neubert and A. Shalapyonok (2003). Growth rates of coastal

Mis en forme : (Asiatique) Chinois (RPC), (Autres) Français (France)

phytoplankton from time-series measurements with a submersible flow cytometer. Limnology and Oceanography 48(5): 1756-1765.

Thyssen, M., N. Garcia and M. Denis (2009). Sub meso scale phytoplankton distribution in the North East Atlantic surface waters determined with an automated flow cytometer. Biogeosciences 6: 569-583.

Thyssen, M., D. Mathieu, N. Garcia and M. Denis (2008b). Short-term variation of phytoplankton assemblages in Mediterranean coastal waters recorded with an automated submerged flow cytometer. Journal of Plankton Research 30(9): 1027-1040.

Thyssen, M., G. A. Tarran, M. V. Zubkov, R. J. Holland, G. Gregori, P. H. Burkill and M. Denis (2008a). The emergence of automated high-frequency flow cytometry: revealing temporal and spatial phytoplankton variability. Journal of Plankton Research 30(3): 333-343.

Uitz, J., H. Claustre, B. Gentili and D. Stramski (2010). Phytoplankton class-specific primary production in the world's oceans: Seasonal and interannual variability from satellite observations. Global Biogeochemical Cycles 24(3): GB3016.

Van Bleijswijk, J. D. L., R. S. Kempers, M. J. Veldhuis and P. Westbroek (1994). Cell and growth characteristics of types A and B of Emiliania huxleyi (Prymnesiophyceae) as determined by flow cytometry and chemical analyses. . Journal of Phycology 30: 230-241.

Van Heukelem, L. and C. S. Thomas (2001). Computer assisted high performance liquid chromatography method development with applications to the isolation and analysis of phytoplankton pigments. Journal of Chromatography A910(1): 31A49.

Vantrepotte, V., H. Loisel, D. Dessailly and X. MÃ©riaux (2012).Optical classification of contrasted coastal waters. Remote Sensing of Environment 123(0): 306-323.

Vargas, M., C. W. Brown and M. R. P. Sapiano (2009).Phenology of marine phytoplankton from satellite ocean color measurements. Geophys. Res. Lett. 36.

Veldhuis, M. J. W. and G. W. Kraay (2000). Application of flow cytometry in marine phytoplankton research: current applications and future perspectives. Scientia Marina 64(2): 121-134.

Waterbury, J. B., S. W. Watson, R. R. L. Guillard and L. E. Brand (1979).Widespread occurrence of a unicellular, marine, planktonic cyanobacterium. Nature 277(293:294).

Werdell, P.J., Proctor, C.W., Boss, E., Leeuw, T. and M. Ouhssain (2013). Underway sampling of marine inherent optical properties on the Tara Oceans expedition as a novel resource for ocean color satellite data product validation. Methods in Oceanography 7: 40-51.

Widdicombe, C. E., D. Eloire, D. Harbour, R. P. Harris and P. J. Somerfield (2010).Long-term phytoplankton community dynamics in the Western English Channel. Journal of Plankton Research 32(5): 643-655.

Wiltshire, K. H. and B. F. J. Manly (2004). The warming trend at Helgoland Roads, North Sea: phytoplankton response. Helgoland marine research 58: 269-273.

Yentsch, C. S. and Menzel, D. W. (1963) A method for the determination of phytoplankton chlorophyll and phaeophytin by fluorescence. Deep Sea Research, 10: 221-231.

Zubkov, M. V. and P. H. Burkill (2006). Syringe pumped high speed flow cytometry of oceanic phytoplankton. Cytometry Part A 69A(9): 1010-1019.

Zubkov, M.V. and G.D. Quartly (2003).Ultraplankton distribution in surface waters of the Mozambique Channel - flow cytometry and satellite imagery. Aquatic Microbial Ecology 33(2): 155-161.

Mis en forme : Interligne : Double

1272 Figure legends:

1273

1274 Figure 1. Flow cytometry sampling points superimposed on the mixed layer depth (m)
1275 calculated with modeled temperature of the water column from the FOAM AMM7 (average
1276 values from the 8 to the 12 May 2011). Chosen stations for phytoplankton pictures collection
1277 with the flow cytometer are labeled (ST=station, ST4, ST6, ST13). Yellow squares correspond
1278 to MODIS matching points for non-turbid waters selected between 6 h and 18 h.

1279 Figure 2. A. Temperature and B. *S*alinity measured with the Pocket Ferry Box.
1280 Presented data are selected to match the scanning flow cytometry collected samples. Grey
1281 bars delimit the traversed marine areas: H= Humber, T=Tyne, D=Dogger, Th=Thames.

1282 Figure 3. A. TFLO vs TFLR (a.u.) cytogram with a trigger level at 10 mV showing the
1283 PicoORG cluster, the PicoRED cluster, the MicroLowORG cluster. B. Maximum SWS (a.u.)
1284 vs TFLR (a.u.) cytogram with a trigger level at 10 mV showing the NanoSWS cluster, the
1285 NanoRED2 cluster and 3 µm beads. C. TFLR (a.u.) vs TFWS (a.u.) cytogram with a trigger
1286 level at 10 mV showing the NanoRED1 cluster, the NanoRED2 cluster, and the Micro1
1287 cluster. D. TFLO vs TLFR (a.u.) cytogram with a trigger level of 25 mV showing the
1288 NanoORG1, the MicroORG, the Micro1 and Micro2 clusters and 10 µm beads. Clusters
1289 colors are consistent across different panels.

1290 Figure 4~~:~~. Pictures of cells from the scanning flow cytometer image in flow device
1291 collected within the Micro2 cluster. Surface closest stations where Micro2 abundance was the
1292 highest (station 4, 6, and 13) are illustrated.

1293 Figure 5~~:~~. Abundance (10^3 cells.cm^{-3}) of each phytoplankton cluster resolved with the
1294 scanning flow cytometer. Scales are not homogenised for the purpose of distribution evidence.
1295 Grey bars separate the traversed marine areas: H= Humber, T=Tyne, D=Dogger, Th=Thames.

Figure 6. Average estimated size for each phytoplankton cluster resolved with the scanning flow cytometer. Scales are not homogenised for the purpose of distribution evidence. Grey bars separate the traversed marine areas: H= Humber, T=Tyne, D=Dogger, Th=Thames.

Figure 7. Scanning flow cytometer Total red fluorescence per unit volume (SFC TFLR.cm^{-3}) for each phytoplankton cluster. Superimposed large black squares are the matching points with MODIS pixels in non-turbid waters between 6 h and 18 h. Diamonds correspond to the night SFC samples matching MODIS passage but not taken into account because of the possible differences between day and night community structures. Scales are not homogenised for the purpose of distribution evidence. Grey bars separate the traversed marine areas: H= Humber, T=Tyne, D=Dogger, Th=Thames.

Figure 8. SFC Total TFLR per cm^{-3} compared to chl a analyses using different instruments. Refer to Material and Methods for a detailed description of each method. Blue triangles: AOA fluorometer PFB (chla µg.dm^{-3}). Black diamonds: SFC Total TFLR.cm^{-3} (a.u..cm^{-3}). Green triangles: Turner fluorometer (chla µg.dm^{-3}). Grey triangles: HPLC (chla µg.dm^{-3}). Red squares: MODIS chla values corresponding to non-turbid waters (after Vantrepotte et al., 2012) and selected between 6 h and 18 h (chla µg.dm^{-3}).

Figure 9~~:~~. A. Within sum of squares for the optimal number of K-nodes selection corresponding to PHYSAT anomalies. B. Cluster dendrogram defining the two main nodes grouping similar PHYSAT anomalies matchups (N1 and N2). C and D, corresponding Ra (Radiance Anomaly) spectra for N1 and N2. Red dashed lines correspond to the minima and maxima values of the spectra as described in Table 3.

Figure 10~~:~~. A and B. Clusters proportional contribution to the Total TFLR.cm^{-3} within each PHYSAT anomaly (N1 and N2). C and D. Within each anomaly, clusters TFLR.cm^{-3} proportional difference to its median value calculated on the entire matching points dataset.

Wilcoxon rank test was run for each cluster between the two anomalies. ***p<0,001, **p<0,01, *p<0,1.

Figure 11~~:~~. Boxplots within each PHYSAT anomaly (N1, N2) of A. Temperature (°C), B. Salinity, C. Chlorophyll *a* (as estimated from MODIS L3 Binned) and D, Total TFLR (a.u..cm^{-3}). Wilcoxon rank test was run for each parameter between the two anomalies. ***p<0,001, **p<0,01, *p<0,1.

Figure 12~~:~~. A and B. Frequency of occurrence of the two distinct anomalies (N1 and N2) over the North Sea during the sampling period (08/05/2011 to the 12/05/2011). Yellow squares correspond to MODIS matching points for non-turbid waters selected between 6 h and 18 h and used to distinguish N1 and N2 PHYSAT anomalies.

Table 1~~:~~. Minimal, maximal, average and standard deviation of abundance (cell.cm^{-3}) for each defined phytoplankton cluster followed by the size estimated (µm) average ± standard deviation values.

Table 2~~:~~. Spearman's rank correlation coefficient between the different methods used for chlorophyll *a* estimates and with the Total TFLR from the scanning flow cytometer per unit volume. ***p<0,001 ** p<0,01.

Mis en forme : Police :Italique

Table 3. Minimal and maximal radiance anomaly (Ra) values for each collected MODIS wavelength (nm) that characterizes the edges for the two PHYSAT radiance anomalies spectra (N1 and N2) observed in this study.

Table 1

Cluster's name	Abundance min-max (cells.cm^{-3})	Average abundance ± SD (cells.cm^{-3})	Average size ± SD (µm)
PicoORG	25 - 18710	1559 ± 2821	1.09 ± 0.17
PicoRED	275 - 26960	5674 ± 4647	1.83 ± 0.32
NanoRED1	97 - 7172	888 ± 942	2.33 ± 0.33
NanoORG	<10 - 759	87 ± 150	5.8 ± 2.1
NanoSWS	< 10 - 376	99 ± 93	10 ± 2.56
NanoRED2	200 - 54880	4187 ± 7878	6.4 ± 1.4
Micro1	<10 - 4392	420 ± 769	16.9 ± 5.6
MicroORG	<10 - 306	48 ± 60	23.5 ± 10
MicroLowORG	<10 - 687	69 ± 111	23.75 ± 8.6
Micro2	<10 - 420	37 ± 59	65.5 ± 21.0

Table 2.

Spearman's correlation coefficient	SFC TFLR.cm^{-3} (a.u.) n=247	AOA fluorometer (µg.dm^{-3}) n=254	HPLC chla (µg.dm^{-3}) n=12	Turner chla (µg.dm^{-3}) n=9
SFC TFLR.cm^{-3} (a.u.)	1	0,93***	0,82***	0,82***
AOA fluorometer (µg.dm^{-3})		1	0,86***	0,82***
HPLC chla (µg.dm^{-3})			1	0,98***
Turner chla (µg.dm^{-3})				1

Table 3.

Node	Ra (412) nm Min	Ra (412) nm Max	Ra (443) nm Min	Ra (443) nm Max	Ra (488) nm Min	Ra (488) nm Max	Ra (531) nm Min	Ra (531) nm Max
N1 (n=5)	1.06	1.30	0.96	1.24	0.91	1.10	0.91	1.09
N2 (n=10)	0.74	0.97	0.75	0.93	0.70	0.89	0.72	0.93

1410

1411

1412 FIGURE 1

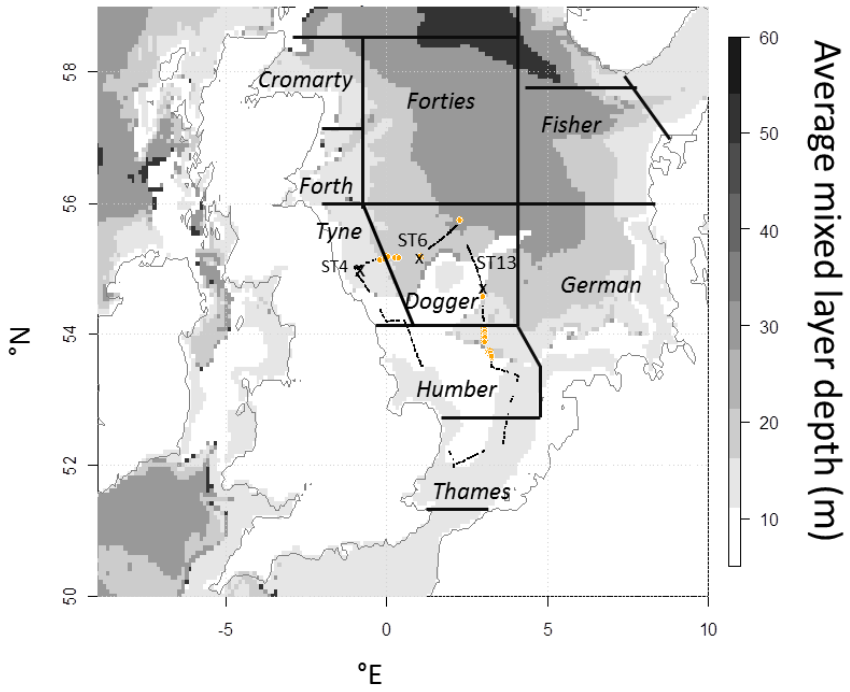

1413

1414

1415

1416

1417

1418

1419

1420

1421

1422

1423

FIGURE 2

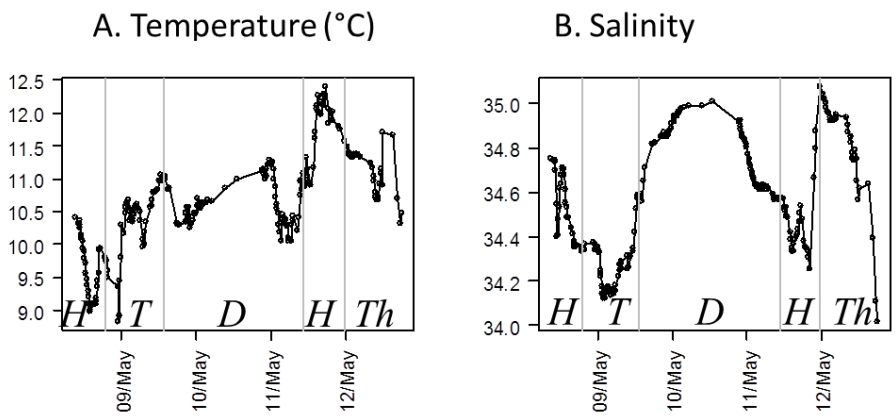
A. Temperature (°C)
B. Salinity
12.5
12.0
11.5
11.0
10.5
10.0
9.5
9.0
35.0
34.8
34.6
34.4
34.2
34.0
H
T
D
H
Th
09/May
10/May
11/May
12/May

FIGURE 3

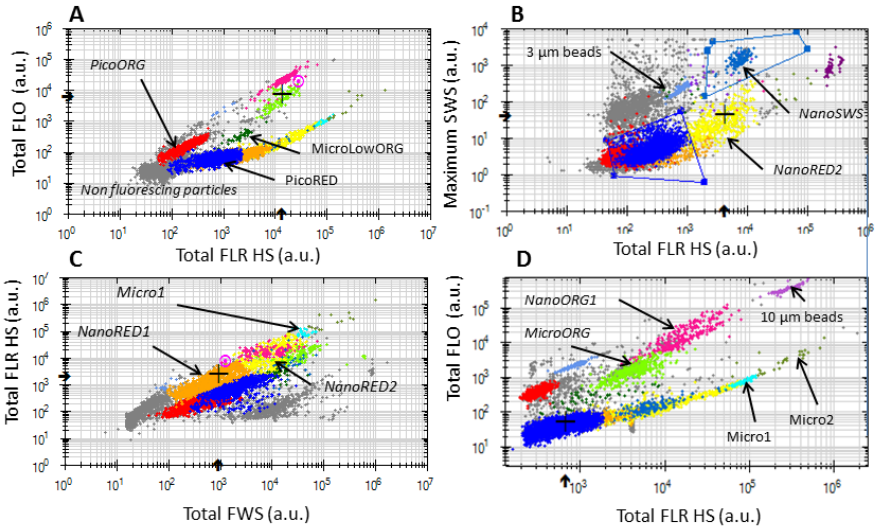
A
PicoORG
MicroLowORG
PicoRED
Non fluorescing particles
Total FLO (a.u.)
Total FLR HS (a.u.)
B
3 µm beads
NanoSWS
NanoRED2
Maximum SWS (a.u.)
Total FLR HS (a.u.)
C
Micro1
NanoRED1
NanoRED2
Total FLR HS (a.u.)
Total FWS (a.u.)
D
NanoORG1
MicroORG
10 µm beads
Micro2
Micro1
Total FLO (a.u.)
Total FLR HS (a.u.)

FIGURE 4

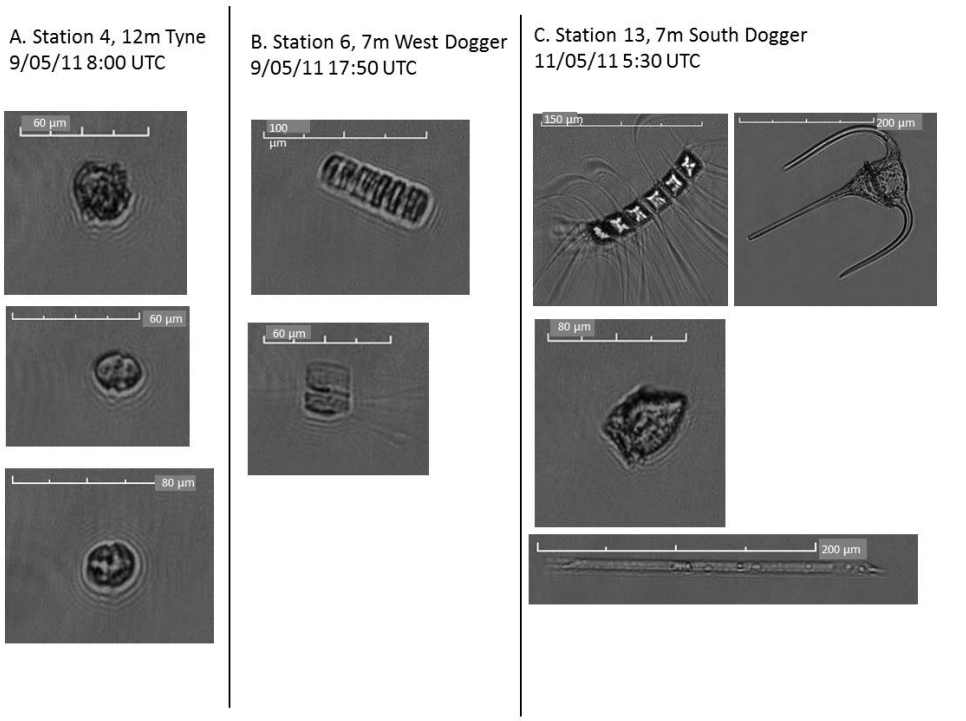
A. Station 4, 12m Tyne
9/05/11 8:00 UTC
B. Station 6, 7m West Dogger
9/05/11 17:50 UTC
C. Station 13, 7m South Dogger
11/05/11 5:30 UTC
60 µm
60 µm
80 µm
100 µm
60 µm
150 µm
200 µm
80 µm
200 µm

1460 FIGURE 5

1461

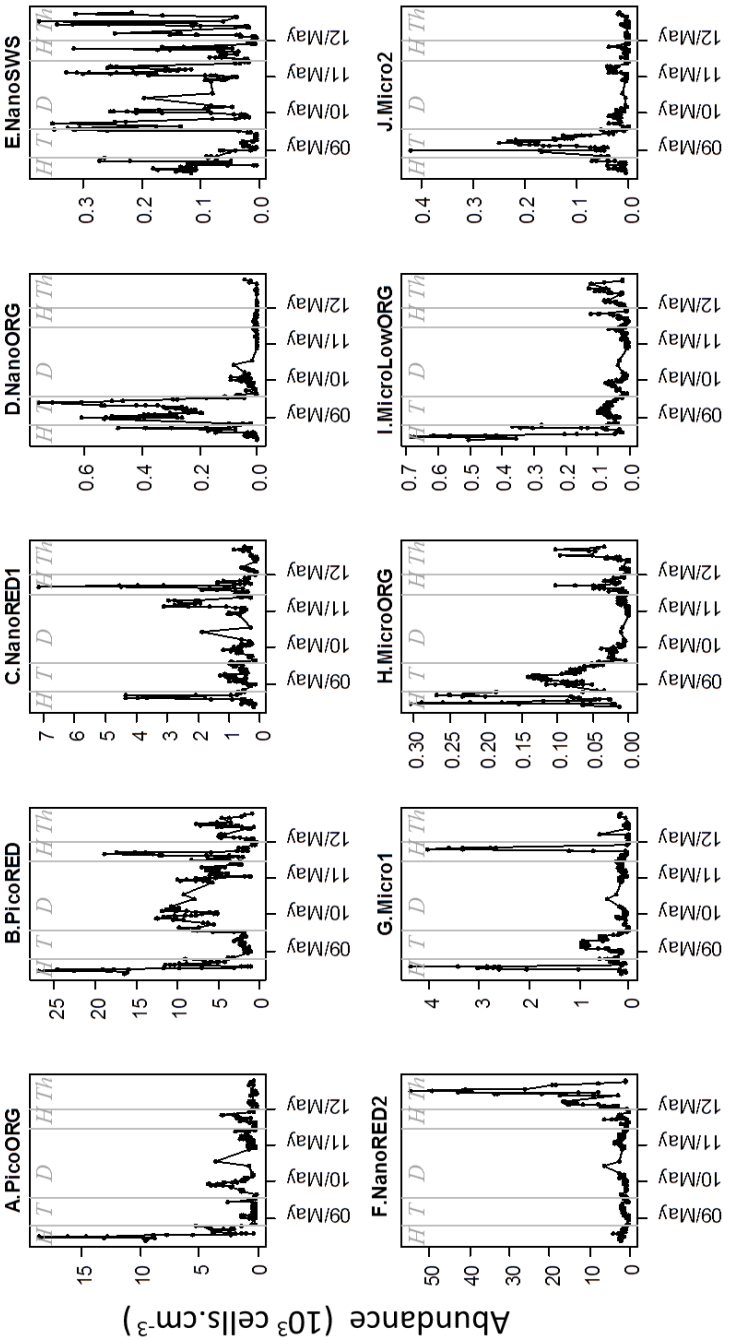

1462

1463 FIGURE 6

1464

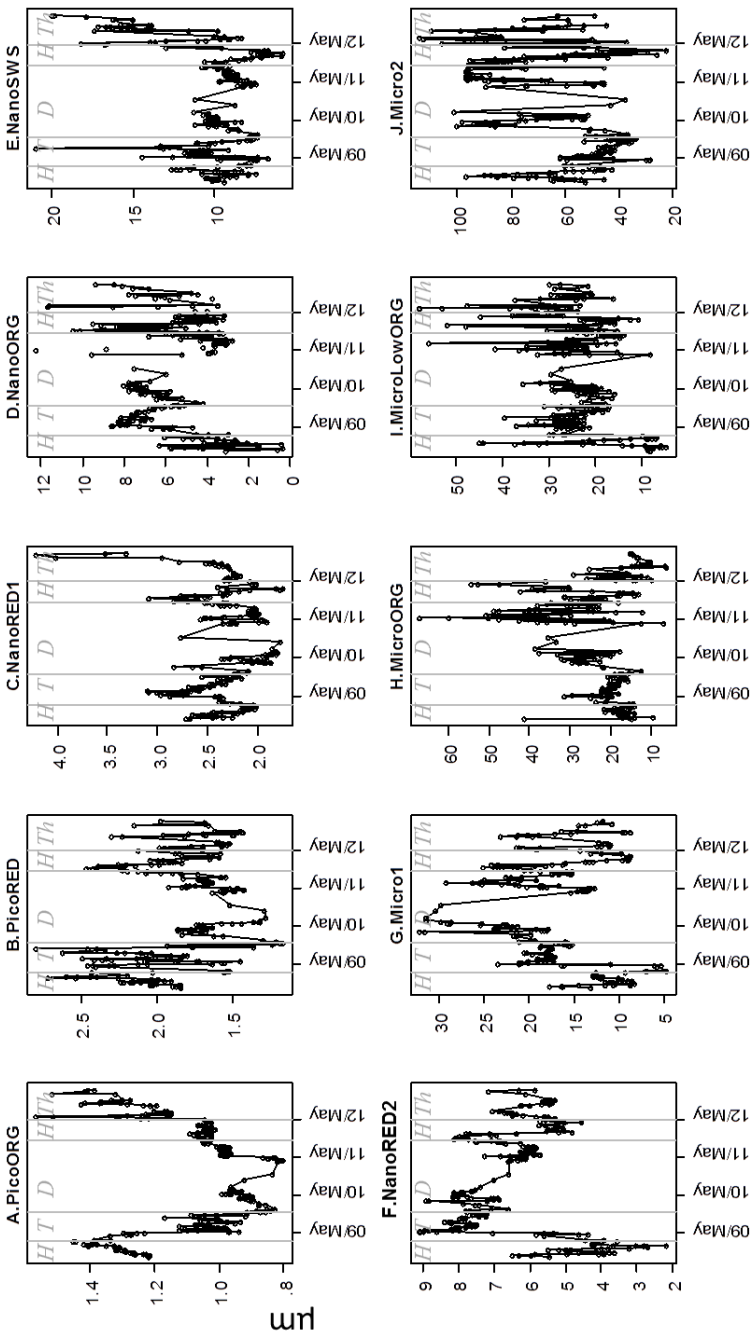

1465

1466 FIGURE 7

1467

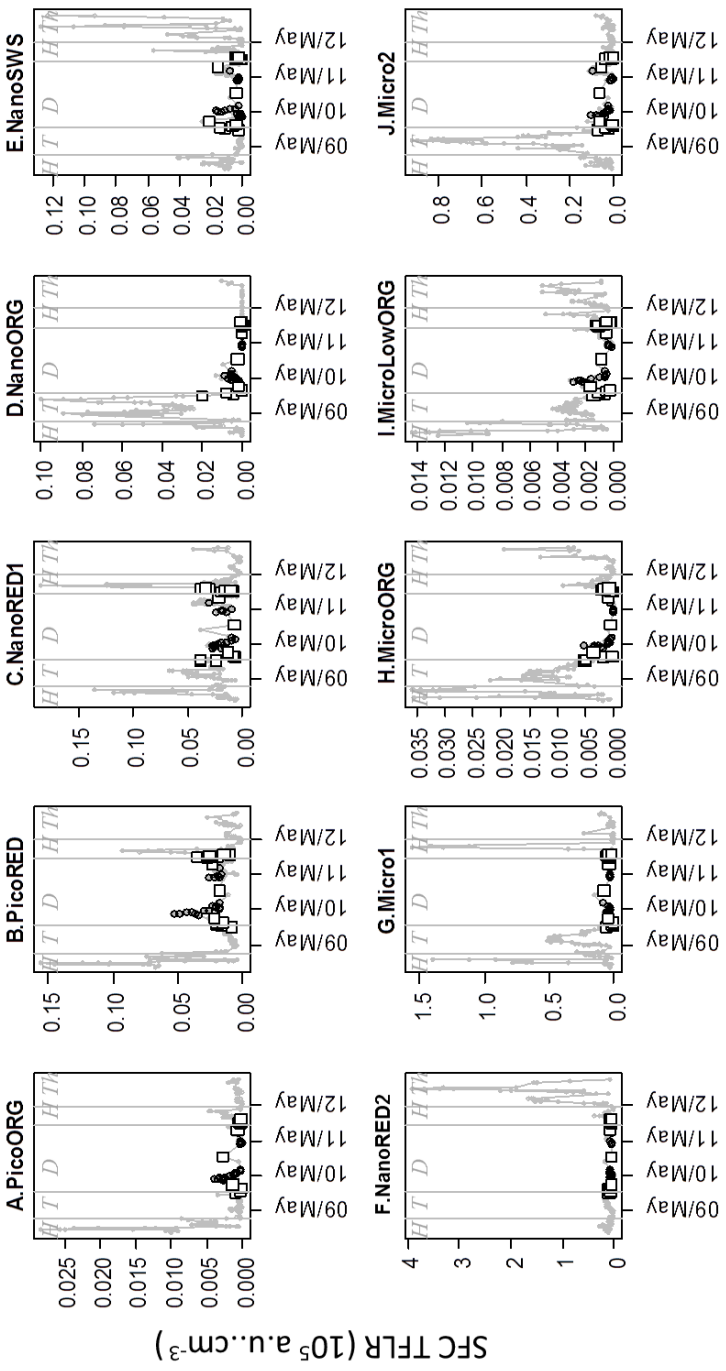

1468

FIGURE 8

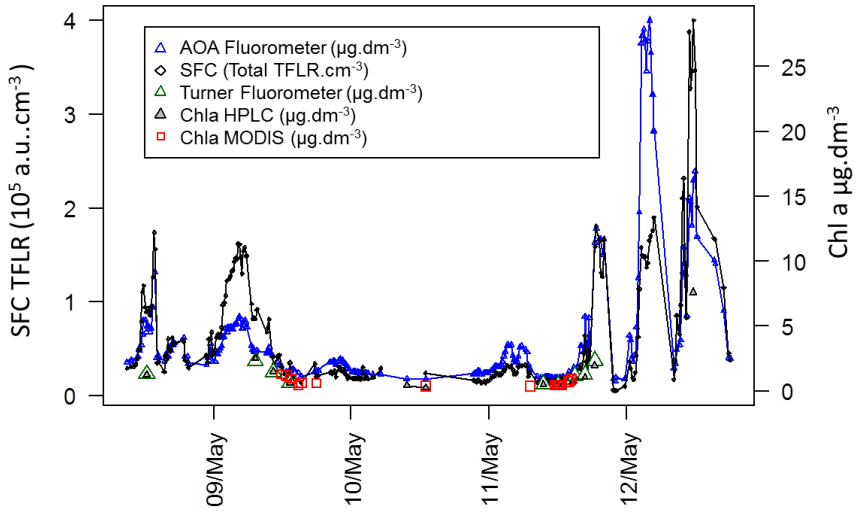
AOA Fluorometer (µg.dm-3)
SFC (Total TFLR.cm-3)
Turner Fluorometer (µg.dm-3)
Chla HPLC (µg.dm-3)
Chla MODIS (µg.dm-3)
SFC TFLR (10^5 a.u..cm-3)
Chl a µg.dm-3
0
1
2
3
4
0
5
10
15
20
25
09/May
10/May
11/May
12/May

FIGURE 9

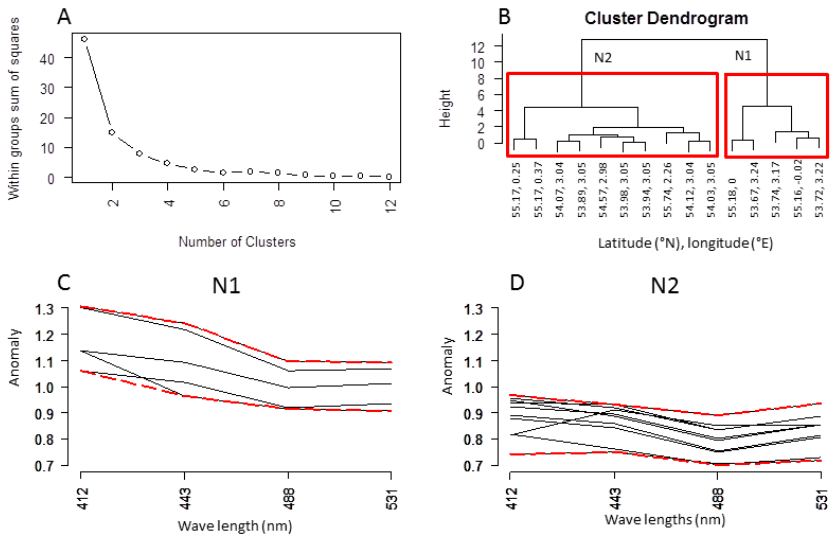
A
Within groups sum of squares
Number of Clusters
B
Cluster Dendrogram
Height
N2
N1
Latitude (°N), longitude (°E)
C
N1
Anomaly
Wave length (nm)
D
N2
Anomaly
Wave lengths (nm)

FIGURE 10

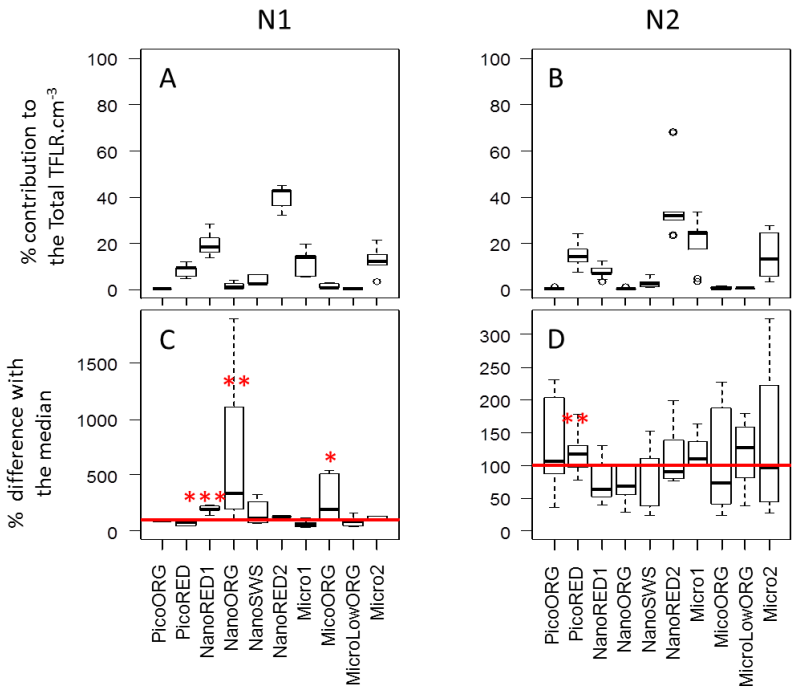

Mis en forme : Taquets de tabulation : Pas à 1.87 cm

FIGURE 11

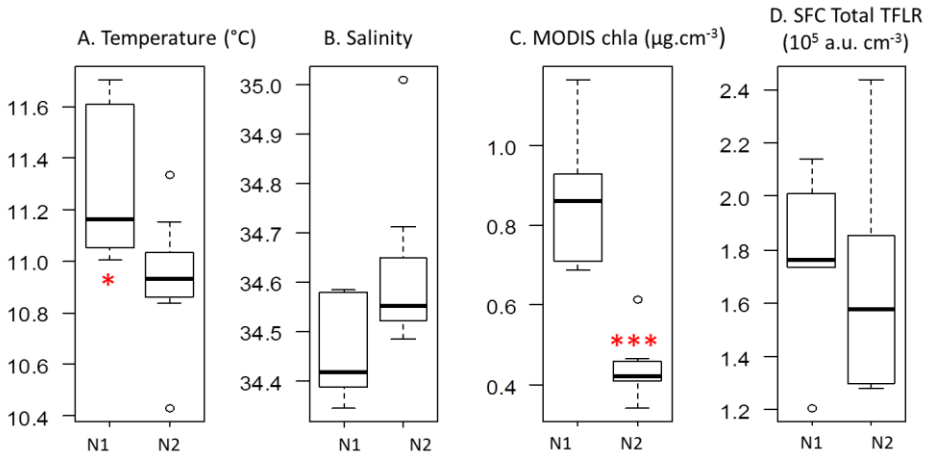
A. Temperature (°C)
B. Salinity
C. MODIS chla (µg.cm-3)
D. SFC Total TFLR
(10^5 a.u. cm-3)
11.6
11.4
11.2
11.0
10.8
10.6
10.4
35.0
34.9
34.8
34.7
34.6
34.5
34.4
1.0
0.8
0.6
0.4
2.4
2.2
2.0
1.8
1.6
1.4
1.2
*
***
N1
N2

Mis en forme : Retrait : Première ligne : 0 cm

FIGURE 12